ISBN 978-82-471-1409-4 (printed ver.)
ISBN 978-82-471-1410-0 (electronic ver.)
ISSN 1503-8181

Doctoral theses at NTNU, 2009:20

Martin Smedstad Foss

The Effect of Oil on Carbon Dioxide Corrosion Inhibition on Carbon Steel - Potential for Improved Corrosion Protection

Martin Smedstad Foss

Doctoral Thesis

NTNU
Norwegian University of
Science and Technology

Thesis for the degree of
philosophiae doctor
Faculty of Natural Science and Technology
Department for Chemical Engineering

Doctoral theses at NTNU, 2009:20

NTNU
Norwegian University of
Science and Technology

NTNU
Norwegian University of
Science and Technology

Martin Smedstad Foss

The Effect of Oil on Carbon Dioxide Corrosion Inhibition on Carbon Steel - Potential for Improved Corrosion Protection

Thesis for the degree of philosophiae doctor

Trondheim, January 2009

Norwegian University of
Science and Technology
Faculty of Natural Science and Technology
Department for Chemical Engineering

NTNU
Norwegian University of
Science and Technology

NTNU
Norwegian University of Science and Technology

Thesis for the degree of philosophiae doctor

Faculty of Natural Science and Technology
Department for Chemical Engineering

ISBN 978-82-471-1409-4 (printed ver.)
ISBN 978-82-471-1410-0 (electronic ver.)
ISSN 1503-8181

Doctoral Theses at NTNU, 2009:20

Printed by Tapir Uttrykk

Preface

This thesis, submitted in partial fulfillment of the requirements for the degree of philosophiae doctor (PhD) at the Norwegian University of Science and Technology (NTNU), consists of five papers which are all based on experimental work carried out at The Institute for Energy Technology (IFE) from August 2004 to November 2007. The work is part of a strategic institute program (SIP) headed by IFE and NTNU and sponsored by the Research Council of Norway (Project no. 158913/I30).

My supervisors throughout this thesis have been Adjunct Professor Egil Gulbrandsen and Professor Johan Sjöblom from the Norwegian University of Science and Technology (NTNU).

Acknowledgements

The first time my supervisor Egil Gulbrandsen reviewed a draft paper I had prepared he explained the significant amount of red markings by telling me he read the paper “like the devil reads the Bible”. I understood what he meant but did not appreciate the full meaning of this until later on. When preparing a scientific document the main teaching is; write enough to get the message across, nothing more. This has later on slowly started to influence the way I prepare manuscripts and has, by my own account, made me a better scientist.

First among the people I want to express my gratitude to is therefore Egil Gulbrandsen. He has been my mentor and my scientific reference point. I would also like to thank Professor Johan Sjöblom, my second supervisor, for his contributions.

I would also like to express my greatest appreciations to everyone working at the Department of Materials and Corrosion Technology at IFE. Marion Seiersten got me started when I came to IFE in 2004, preparing me for the PhD I later started on. The senior scientist staff at the Department of Materials and Corrosion Technology was when I started, and continue to be, academically inspiring, always being part of the cutting edge in our field of research.

Apart from the people helping me in an academic sense, there are some others that I want to give thanks to. My mother and father helped make me the man that I am, sowing the academic seed that lead me to where I am professionally. An invaluable contribution has also been made by my good friend, Øystein, through countless hours on the phone during these last 4 years.

I would also like to thank my wife, Synne, and my two small stress relievers, Heine and Ylva. They are the guiding light in my life.

Abstract

The search for robust and cost efficient ways to prevent internal corrosion of carbon steel piping and equipment in oil and gas production and transportation has lead to the development of highly sophisticated CO_2 corrosion inhibitor products. This thesis studies oil wetting and corrosion inhibitor performance on bare steel and steel with corrosion product deposits on the surface, in the presence of a refined, low aromatic hydrocarbon oil. Three surfactants were used in the experiments; two commercial inhibitor base chemicals; an oleic imidazoline salt (OI) and a phosphate ester (PE), and cetyl trimethyl ammonium bromide (CTAB), a well characterized quaternary ammonium compound. Adsorption characteristics of the inhibitors on corroding iron and $FeCO_3$ particles were also studied.

Polarization resistance (PR) and electrochemical impedance spectroscopy (EIS) techniques were used to study the effect of the oil on the performance of the inhibitors. The performance testing was done on corroding carbon steel without any surface deposits and on carbon steel with either ferrous carbonate ($FeCO_3$) or ferric corrosion products on the surface. The results showed that the addition of oil in the inhibitor tests had a significant, positive effect on the performance of the two commercial corrosion inhibitors; decrease in corrosion rate of about one order of magnitude compared to the rate without oil was found. Based on the EIS data it was concluded that the improved performance was caused by a modification of the inhibitor film and not the formation of a macroscopic oil film on the steel surface. Indications of oil wetting of the steel surface were only found when ferric corrosion products were present and OI was used as the inhibitor. No such effects were seen on bare steel or on $FeCO_3$ covered surfaces.

Contact angle measurements and dispersion tests were used to investigate the effect of the inhibitors on the wettability of the three types of surfaces when they were exposed to water and oil. Both the behavior of an oil droplet on an already water-wet surface and a water droplet on an already oil wet surface were investigated to determine the ability of the inhibitors to alter the affinity of the surface to water and oil respectively. The results indicated the no hydrophilic to hydrophobic transition occurred on bare steel and $FeCO_3$ covered steel. The testing on surfaces with ferric corrosion products revealed that a water-

wet to oil-wet transition was possible on the ferric deposits using both PE and OI as inhibitor. The effect was, however, significantly stronger with OI than with PE. It was also found that the addition of the two inhibitors enhanced the hydrophobic behavior of an already oil-wet surface for both bare steel and steel with $FeCO_3$ deposits. Water droplets entrained in the oil was in these experiments not able to spread on the steel surface.

Electrophoresis measurements were used to determine influence of the three inhibitors on the zetapotential of $FeCO_3$ and corroding iron particles. The tendency of the inhibitors to adsorb on surfaces with the same charge as the head group of the inhibitor was investigated. The focus in the testing on corroding iron was to determine the suitability of zetapotential as a method for investigating surface potential of corroding surfaces. It was found that the inhibitors adsorbed on iron carbonate regardless of the surface charge on the iron carbonate. On iron particles the experiments indicated that measurements of the surface potential of corroding particles could only be done when the corrosion rate had been reduced significantly using corrosion inhibitors.

List of Publications

Journal Papers

1. M. Foss, E. Gulbrandsen, J. Sjöblom, ”Alteration of Wettability of Corroding Carbon Steel Surface by CO_2 Corrosion Inhibitors. The Effect on CO_2 Corrosion Rate and Contact Angle”, Corrosion 64 (2008), p. 905.

2. M. Foss, E. Gulbrandsen, J. Sjöblom, ”Effect of Corrosion Inhibitors and Oil on Carbon Dioxide Corrosion and Wetting of Carbon Steel with Ferrous Carbonate deposits”, Corrosion 65 (2009), p. 3.

3. M. Foss, E. Gulbrandsen, J. Sjöblom, ”CO_2 Corrosion Inhibition and Oil Wetting of Carbon Steel with Ferric Corrosion Products”, Corrosion, Submitted

4. M. Foss, E. Gulbrandsen, J. Sjöblom, ”Adsorption of Corrosion Inhibitors onto Iron Carbonate ($FeCO_3$) Studied by Zetapotential Measurements”, Journal of Dispersion Science and Technology 30 (2009), 10/21.

5. M. Foss, E. Gulbrandsen, J. Sjöblom, ”Measurements of zeta potential on corroding, high-purity iron particles: influence of corrosion inhibitors”, Journal of Dispersion Science and Technology 30 (2009), 10/26.

Conference papers

1. M. Foss, E. Gulbrandsen, J. Sjöblom, ” CO_2 corrosion inhibition and oil wetting of carbon steel with ferric corrosion products”, Paper no.05914, National Association of Corrosion Engineers (NACE) CORROSION/09 Conference (2009).

2. M. Foss, E. Gulbrandsen, J. Sjöblom, ” Interaction of Carbon Dioxide Corrosion Inhibitors with Corrosion Products Deposit”, Paper no.08343, National Association of Corrosion Engineers (NACE) Corrosion/08 Conference (2008).

3. M. Foss, E. Gulbrandsen, J. Sjöblom**,** ”The effect of corrosion inhibitors on the wettability and CO_2 corrosion rate of carbon steel” **1**8th Oil Field Chemistry Symposium 2007, 25. - 28. March 2007, Tekna - Norwegian Society of Chartered Technical and Scientific Professionals.

4. M. Foss, E. Gulbrandsen, J. Sjöblom, “Modification of wettability of corroding carbon steel surface by CO corrosion inhibitors, and its effect on CO corrosion rate”, Eurocorr 2006, European Federation of Corrosion (EFC), Maastricht, The Netherlands, September 2006.

5. M. Foss, K. Bilkova, E. Gulbrandsen, M. Knag, J. Sjöblom, “Interaction of CO_2 corrosion inhibitors with corrosion product deposits.”, Proceedings of the 10th European Symposium on Corrosion and Scale Inhibitors (10 SEIC), Ann. Univ. Ferrara, N.S., Sez. V, Suppl. N. 12, p. 601, 2005. Ferrara, Italy, 2005.

Contents

1 Introduction

Carbon steel pipelines are commonly employed in the transport of oil and gas. Carbon steel piping and process equipment are subject to corrosion caused by the presence of water and acidic gases such as carbon dioxide (CO_2), hydrogen sulfide (H_2S) and acetic acid (CH_3COOH). The water-cut in the production stream might vary, but, even small amounts of acidic water might cause severe internal corrosion of carbon steel used in the production equipment. The corrosiveness of the aqueous phase is determined by many parameters, such as the pH, temperature, water chemistry and presence of dissolved hydrocarbons.[1] In addition to these parameters the distribution of the water in the stream (e.g. stratified or dispersed flow pattern), and to which extent the aqueous phase actually is wetting the steel surface, affect the corrosion risk of the system. The former factor is a topic of multiphase flow hydrodynamics; the latter is a topic of surface chemistry. The use of corrosion inhibitors and the manipulation of corrosion product films are two possible ways of lowering the corrosion rate to acceptable levels.[2,3]

Corrosion inhibitors are widely used in the oil and gas industry to protect carbon steel piping from internal corrosion. The mechanism of inhibition of CO_2 corrosion is not well understood. However, the self assembled hydrocarbon chains form structures with hydrocarbon phase properties that may change electrochemical reaction rates, influence the mass transfer of reactants or reaction products, or simply block parts of the surface, and thus reduce the active area.[3] Previous inhibitor testing work has demonstrated that the performance of CO_2 corrosion inhibitors in many cases was reduced when the steel was corroded before inhibition.[4] The presence of $FeCO_3$ deposits might also influence the ability of the inhibitor to access the surface, thereby reducing the effective performance of the corrosion inhibitor. Limited data has yet been published on the interaction between this partly protective corrosion deposit and corrosion inhibitors.[5,6]

Oil wetting and corrosion inhibitor performance on bare steel and steel with surface deposits in the presence of a refined, low aromatic hydrocarbon oil was investigated. Three surfactants were used in the experiments; two commercial inhibitor base chemicals and a well characterized surfactant. The two corrosion inhibitors, an oleic imidazoline (anionic)

and a phosphate ester compound (cationic), were chosen based on their corrosion inhibiting properties.[7,8] The general surfactant, cetyl trimethyl ammonium bromide (CTAB), was included as a reference surfactant. A special focus has been on the possibility of changing the wettability of a steel surface with ferrous or ferric corrosion product deposits, thereby lowering the corrosion rate of the steel significantly. Both electrochemical methods, such as polarization resistance and electrochemical impedance spectra, and common methods for wetting evaluation, such as contact angle and dispersion testing, have been used in the study. In addition to the performance and wettability testing the adsorption of the inhibitors onto $FeCO_3$ and iron particles was investigated. The influence of oil and surface charge on the adsorption isotherm for the inhibitors and the feasibility of using electrophoretic measurements to investigate adsorption of corrosion inhibitors on corroding iron were also investigated.

2 Surfactants and surfaces in aqueous solutions

The understanding of the solid-liquid interface and how surfactants interact with this interface is essential to the understanding of corroding surfaces. The influence of surface charge, pH, electrolyte composition and the structure of the double layer are some of the main factors that should be understood. The following sections discuss some of the basic theories and effects involved in surface science.

2.1 The electrical double layer

The double layer theory is a simplified model of the potential near the interface between two phases, such as a metal surface and an aqueous solution. Ions and polarized molecules present in the solution will distribute in a non-uniform way close to the surface of the solid. Near the surface an excess of ions will accumulate and form a layer.[9] This formation of a charged interface greatly affects how molecules present in the solution interact with the solid surface. In the theory below it is assumed that no diffusion of charge across the interface if the potential across the interface is changed. This means that the behaviour of the electrode-solution interface is analogous to that of a capacitor. A brief summary of the main theories leading up to the current models for the charged interface is given below.

2.1.1 Models for double layer structure

To establish a model describing the double layer in detail various approaches have been used. The simplest model is the flat plate model. Here, it is assumed that the surface can be treated in a one-dimensional model, leading to the simplification of the geometrical factors involved. The flat plate model was developed by Gouy and Chapman in independent studies.[10] The model introduces the concept of a diffuse layer of ions, which they attempted to describe through a statistical mechanical approach.

Gouy and Chapman divided the layer of ions adjacent to a surface into lamellae and used the knowledge that the electrostatic potential (ψ) varies throughout the layer to calculate the potential distribution.

If charged ions are distributed evenly on a surface to form a layer, a fundamental electrostatic equation called the *Poisson equation* (2.1) can be used to describe how the electrostatic potential (ψ) varies with the distribution of charge ($\rho_v\left(\vec{r}\right)$).[11]

$$\nabla^2\psi\left(\vec{r}\right) = -\frac{\rho_v\left(\vec{r}\right)}{\varepsilon} \tag{2.1}$$

Where ε is the dielectric permittivity *(F m^{-1})*, ∇^2 is the Laplace operator[12], ψ is the electrostatic potential (V) and ρ_v is the volume density of charge (*C m^{-3}*). If permittivity is independent of position equation (2.1) is given in Cartesian coordinates as (2.2):

$$\nabla^2\psi\left(\vec{r}\right) = -\left(\frac{1}{4\pi\varepsilon_0}\right)\times\frac{4\pi\rho_v\left(\vec{r}\right)}{\left(\frac{\varepsilon}{\varepsilon_0}\right)} \tag{2.2}$$

Where ε_0 is the dielectric permittivity of free space. In order for this equation to be valid it is assumed that the surface is equipotent. For the system to be in equilibrium the chemical potential (μ *(J $mole^{-1}$)*) of the ions must be constant *($\nabla\mu_i = 0$)*. The electrical and diffusional forces must therefore cancel each other out:

$$\nabla\mu_i\left(\vec{r}\right) = -z_i e\nabla\psi\left(\vec{r}\right) \tag{2.3}$$

Where ∇ is the vector differential operator[12], e is the elementary charge and z_i is the valence of the ion, i. When considered only in the x direction this reduces to:

$$\frac{d\mu_i}{dx} = -z_i e\frac{d\psi}{dx} \tag{2.4}$$

This equation can be combined with the definition of the chemical potential:

$$\mu_i = \mu_i^0 + kT\ln n_i \tag{2.5}$$

Where n_i is the number of ions, k is the Boltzmann constant and μ^0_i is the standard chemical potential.[9] The combined equation can then be integrated from a point in the bulk

solution where the charge is zero and the concentration of ions equals n_i^0 to form the *Boltzmann equation* (2.7):

$$\int_{n=n_i^o}^{n=n_i} \frac{1}{n_i} dn_i = -\int_{\psi=0}^{\psi=\psi} \frac{z_i e}{kT} d\psi \tag{2.6}$$

$$n_i = n_i^{\,0} \exp\left(\frac{-z_i e\psi}{kT}\right) \tag{2.7}$$

This equation gives the local concentration of each type of ion in the double layer region. The volume density of charge close to the surface is then given by (2.8):[9]

$$\rho_v = \sum_i n_i z_i e \tag{2.8}$$

A combination of equation (2.2), (2.7) and (2.8) then yields the complete *Poisson-Boltzmann equation* (2.9):

$$\nabla^2\psi = \frac{d^2\psi}{dx^2} = -\left(\frac{1}{4\pi\varepsilon_0}\right) \times \frac{4\pi}{\left(\frac{\varepsilon}{\varepsilon_0}\right)} \times \sum_i n_i^{\,0} z_i e \exp\left(\frac{-z_i e\psi}{kT}\right) \tag{2.9}$$

This is the fundamental equation describing the double layer. The equation can be solved analytically but most solutions used are approximations based on some simple assumptions. The equation above is in Cartesian coordinates. The Gouy-Chapman approach to this was to assume a symmetrical electrolyte where the concentrations of positive and negative charges are equal (which means that the valency *z* can be set equal to the valency of the ions that are accumulated in the double layer.[9]) and introducing border criteria for the Poisson-Boltzmann equation.[10] Equation (2.9) can then be written in the form:

$$\frac{d^2\psi}{dx^2} = \left(\frac{1}{4\pi\varepsilon_0}\right) \times \frac{8\pi n_i^0 z_i e}{\left(\frac{\varepsilon}{\varepsilon_0}\right)} \times \sinh\left(\frac{z_i e\psi}{kT}\right) \tag{2.10}$$

By integration the expression is reduced to:

$$\tanh\left(\frac{z\widetilde{\psi}}{4}\right) = \tanh\left(\frac{z\widetilde{\psi_0}}{4}\right)\exp\left(-\kappa x\right) \tag{2.11}$$

where $\widetilde{\psi} = \frac{e\psi}{kT}$ is a dimensionless potential parameter, ψ_0 is the electrostatic potential at the surface and

$$\kappa = \left(\frac{e^2 \sum_i n_i^0 z_i^2}{\varepsilon kT}\right)^{\frac{1}{2}} \tag{2.12}$$

κ is called the *Debye-Hückel* parameter and describes an important relationship in colloid chemistry. The distance 1/κ is often referred to as the double layer thickness although this is not always correct. Equation (2.11) is a general approximation of the double layer where the only assumption made is that $\psi_0 << \frac{4}{z}$. This approximation is usually followed when calculating surface potential. The solutions to the reduced Poisson-Boltzmann equation form the basis for the *diffuse layer theory*. By assuming a very low potential in the double layer region *($z_i e\psi << kT$)*, the simplified Taylor series expansion of the exponential function e^x, $e^{-x}=1-x$, can be used. If this is combined with the knowledge that electro neutrality must be fulfilled a simplified equation (2.13) can be presented:

$$\psi = \psi_0 e^{-\kappa x} \tag{2.13}$$

Which is exponential with a limit for a small ψ_0 and a good approximation when $\psi_0 < \frac{50mV}{z_i}$, at 25 degrees Celsius.[10] This approximation is, however, not valid for most colloidal systems.[9]

Equation (2.13) describes how the potential drop in the diffuse double layer propagates as the distance from the interface increases. The double layer theory was developed further by the realization that the charges in the double layer could not be regarded as point charges. This realization was reached through calculations determining the differential capacitance of the interface. The capacitance in the Gouy-Chapman system yielded increasingly unrealistic values when the potential of the surface itself moved away from an uncharged state. A new concept with a plane of closest approach was therefore introduced by Stern. [13] T*he diffuse double layer is therefore split in two regions, one inner compact layer and one diffuse outer layer*. A schematic drawing of this is seen in Figure 2.1. The layout of the inner layer is determined chiefly by geometry of the ions and short-range interactions. The diffuse outer layer can then be expected to behave according to the Poisson-Boltzmann equation. Stern proposed a theory where the innermost ions (located at the inner Helmholtz plane) interact with the surface of the material through a specific chemical adsorption potential *(ψ_{ads})*. The ions outside this layer are treated as if they are located some distance from the surface, at the outer Helmholtz plane. This procedure amounts to treating the layers as molecular capacitors with sharp changes in permittivity between successive pairs of plates. The principal effect in introducing the compact layer is to lower the overall capacitance of the interfacial region, giving a better representation of the interface.

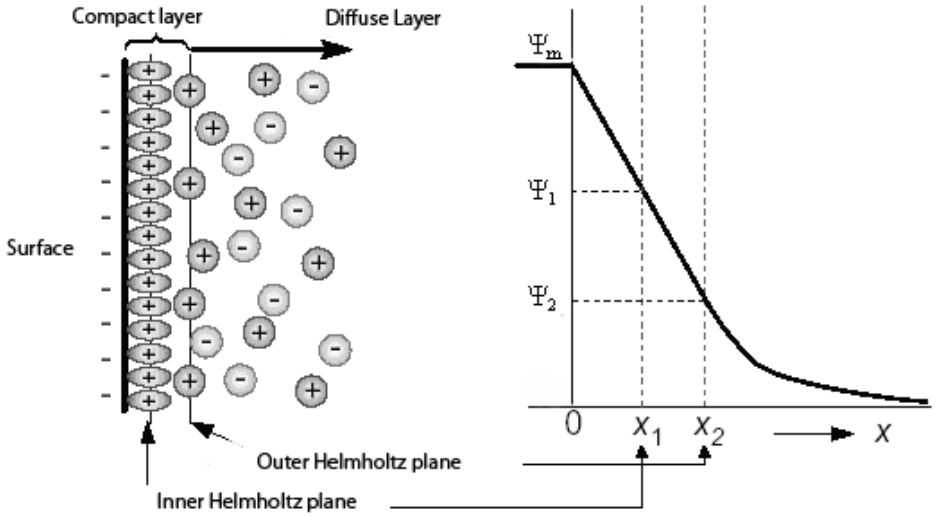

Figure 2.1. Simple representation of the electrical double layer emerging from the Stern modification to the Poisson-Boltzmann theory. The inner Helmholtz plane lies at X_1, the outer Helmholtz plane lies at X_2. ψ_m is the potential at the metal surface.[14]

The Stern-Gouy-Chapman model presented above is a central concept in surface chemistry and corrosion science. If ions are introduced into a system with a developed double layer it becomes clear that the evaluation of electrical interactions between the ion and the ions in the electrical double layer might be important when studying the system

In many cases the solid surfaces that should to be evaluated are often small spherical particles and not flat plates. A theoretical overview of the main theories describing the double layer on a curved surface is therefore of interest. The Poisson-Boltzmann equation (2.9) remains true for a spherical particle. Using the Laplace operator for spherical coordinates, and assuming a spherically symmetric potential, we get:

$$\nabla^2\psi = \frac{1}{r^2}\frac{d}{dr}\left(r^2\frac{d\psi}{dr}\right) = -\frac{1}{\varepsilon}\times\sum_i n_i^{\,0} z_i e \exp\left(-z_i\tilde{\psi}\right) \qquad (2.14)$$

This equation cannot be solved analytically like the Gouy-Chapman solution for the flat plate. Reduced expressions like the Debye-Hückel approximation, valid only for small values of the potential, are therefore used instead. A solution for potential distribution can then be found as:

$$\psi = \psi_0 a \frac{e^{-\kappa(r-a)}}{r} \tag{2.15}$$

where r is the distance from the centre of the sphere, a is the radius of the particle. This solution assumes that the ions are point charges, and it thus not a valid equation for most systems. Attempts have been made to reach a numerical solution to the Poisson-Boltzmann for a particle but the equations will not be reproduced here.[15-17]

2.1.2 The surface density of charge – linking zetapotential to surface charge of particles

At equilibrium, the charge on a surface balances that of the adjacent solution. By integrating the potential from the surface and out into the bulk of the solution an expression for the charge per unit area of the surface (σ_0) can be found (2.16).

$$\sigma_0 = -\int_0^\infty \rho_v dx \tag{2.16}$$

Assuming a symmetrical solution and substituting for ρ_v, the equation reduces to equation (2.17).

$$\sigma_0 = 4\frac{n_i z_i e}{\kappa}\sinh\left(\frac{z_i \widetilde{\psi}_0}{2}\right) \tag{2.17}$$

It is now useful to introduce the term Zetapotential (ξ). The zetapotential is the potential at the shear plane between the rigid part of the double layer and the surrounding solution. At this plane the potential is called the zetapotential ($\psi = \xi$). Inside the shear plane the ions of the double layer are held in place by the surface charge distribution, outside the shear plane the ions follow the movement of the surrounding solution. If this plane is used as a limit for the integral of equation (2.17) an expression for the net charge per unit area over

the shear plan can be found. This can be called the electrokinetic charge density (σ_e) and is given in equation (2.18) for a symmetrical electrolyte.

$$\sigma_e = 4\frac{n_i z_i e}{\kappa}\sinh\left(\frac{z_i \xi_r}{2}\right) \tag{2.18}$$

where $\xi_r = \frac{e\xi}{kT}$, is the dimensionless zetapotential. σ_e can be multiplied with the surface area to obtain the electrophoretic charge (Q_e). By using this relationship it is thus possible to determine Q_e based on measurements of the zetapotential.

For a spherical particle an equivalent expression for the electrokinetic charge density can be derived from equation (2.14). Since no exact solution to the equation is possible an expression based on the Debye-Hückel approximation (ka<<1) is possible. For a symmetrical electrolyte this yields:

$$\sigma_e A = \left(4\pi\varepsilon_0\right)\left(\frac{\varepsilon}{\varepsilon_0}\right)a\left(1+\kappa a\right)\xi \tag{2.19}$$

Work by Stigter showed that the electrophoretic charge calculated using equation (2.19) was reasonable accurate for 0<<κa<1.[9]

The inaccuracy of equation (2.19) is, however, significant for κa>1. Loeb et al. derived an analytical approximation to the Poisson-Boltzmann equation for spherical particles based on an empirical relationship.[17] The accuracy of the solution is within 1 % in most cases where the product of the Debye-Hückel parameter (κ) and the diameter of the sphere (a) is larger than 1, κa>11.[9] This empirical relationship is given in equation (2.20).

$$Q_e = 4\pi\varepsilon_0\left(\frac{\varepsilon}{\varepsilon_0}\right)\frac{kT}{ze}\kappa a^2\left\{2\sinh\left(\frac{z\xi_r}{2}\right)+\frac{4}{\kappa a}\tanh\left(\frac{z\xi_r}{4}\right)\right\} \tag{2.20}$$

Where

$$\kappa = \left(\frac{2000F^2}{\varepsilon_0 \left(\frac{\varepsilon}{\varepsilon_0} \right) RT} \right)^{1/2} \times \sqrt{I} \tag{2.21}$$

$$I = \frac{1}{2} \sum c_i z_i^2 \tag{2.22}$$

In the above equations ε_0 is the relative permittivity in vacuum, c_i is the concentration of the ion of valence z_i, F is the Faraday's constant and ξ is the zetapotential on the particle. This relationship can then be used to convert recorded values for zetapotential to electrophoretic charge of the particle as a whole.

2.2 Surfactants in aqueous environments

Surfactants are a class of more or less water soluble chemicals exhibiting two key properties. First they have a strong tendency for self-assembly in solution and secondly they have a strong affinity to surfaces and interfaces. These properties are evident even at low concentrations.[3,18] The chemicals are typically amphiphilic with a distinct hydrophobic (oil-soluble) and a distinct hydrophilic (water-soluble) part of the molecule. The hydrophobic part often consists of a hydrocarbon chain of some length (C8-C18), possibly with branching or aromatic components. The hydrophilic part of the molecule, often referred to as the head group, is either an ionic group or built up of a number of electrophilic or nucleophilic constituents (typically centred on a double bonded nitrogen or oxygen atom). Surfactants can be classified by the nature of the hydrophilic part of the molecule.[19] The four types of surfactants are given in Table 2.1.

Table 2.1. The four types of surfactants classified by the nature of the hydrophilic part of the molecule.

Type of surfactant	**Key feature**
Anionic surfactants	-The head group of the molecule has a negative charge
Cationic surfactants	-The head group of the molecule has a positive charge
Zwitterionic surfactants	-The head group can have both negative and positive charge
Non-ionic surfactants	-The head group has no charge

The anionic, cationic and zwitterionic molecules that depend on protonation are strongly affected by the solution pH. As shown in the Henderson-Hasselbach equation (2.23) it is clear that protonation of head groups are strongly dependent on pH and they might therefore be non-ionic or ionic depending on the pH of the system.[11]

$$pH = pK_a - \log\left(\frac{[Acid]}{[Base]}\right) \tag{2.23}$$

pK_a is the acidity constant of the compound. Ionic surfactants with a permanent charge, like sodium dodecyl sulphate, remain soluble in water though a wider pH range. The solubility of the surfactant depends strongly on the hydrocarbon chain (R) in addition to the ionic nature of the head group. The length of the hydrocarbon chain is therefore limited by the need for a certain solubility (less soluble for longer R chains) and the effectiveness as a surfactant (less surface active for shorter R chains). Some examples of the molecular structure and uses of surfactants are given in Figure 2.2 and Table 2.2.

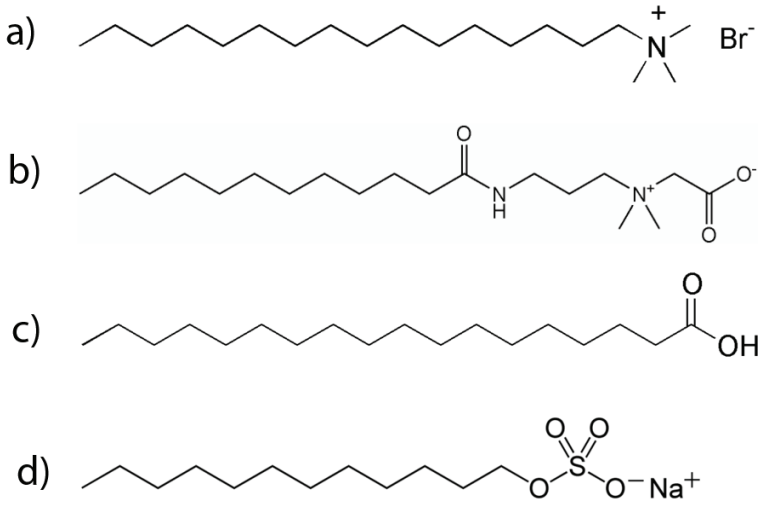

Figure 2.2. Examples of common surfactants. a) cetyl trimethyl ammonium bromide b) Cocamidopropyl betaine-2 c) Stearic acid d) sodium dodecyl sulphate (SDS).

Table 2.2. Examples of surfactant groups and typical applications for the surfactants.

Surfactant	**Head group**	**Alkyl chain (R)**	**Application**
SAS (Anionic)	$SO_3^-Na^+$	CH_3-$(CH_2)_n$-	Detergent
SDS (Anionic)	$SO_4^-Na^+$	CH_3-$(CH_2)_n$-	Detergent, Gel-former
Imidazolines (Cationic)	$C_3(R'/R'')HN_2(R''')$	CH_3-$(CH_2)_n$- / R'' / R'''	Corrosion inhibitors, dispersants
Fatty acids (Non-ionic)	(R)COOH	CH_3-$(CH_2)_n$-	Detergents
Salts of fatty acids (Anionic)	$(R)COO^-M^+$	CH_3-$(CH_2)_n$-	Surfactants in oil/water
Amino acids (Zwitterionic)	H_2N^+-CH(R)-COO^-H^+	CH_3-$(CH_2)_n$- / Complex R-	Dispersant, biocide

2.2.1 Self assembly and Critical Micelle Concentration (CMC)

Surfactant solutions also exhibit some essential features that are typical for each individual surfactant. One such feature is the critical micelle concentration (CMC). At low concentrations amphiphilic molecules usually exist as free monomers in solution. At a certain concentration aggregates, consisting of several surfactant monomers, form. This spontaneous reaction is called self assembly and the resulting, structured aggregates are called micelles. Further addition of surfactant does not lead to increased monomer concentration in solution but instead increase the amount of surfactant in the micelles or the number of micelles. When properties such as conductivity, surface tension and osmotic pressure are plotted as a function of concentration a sharp change in the effect of concentration is seen when the CMC is reached. Figure 2.3 illustrates how some of the characteristic properties of the solution change when the concentration reaches the CMC.

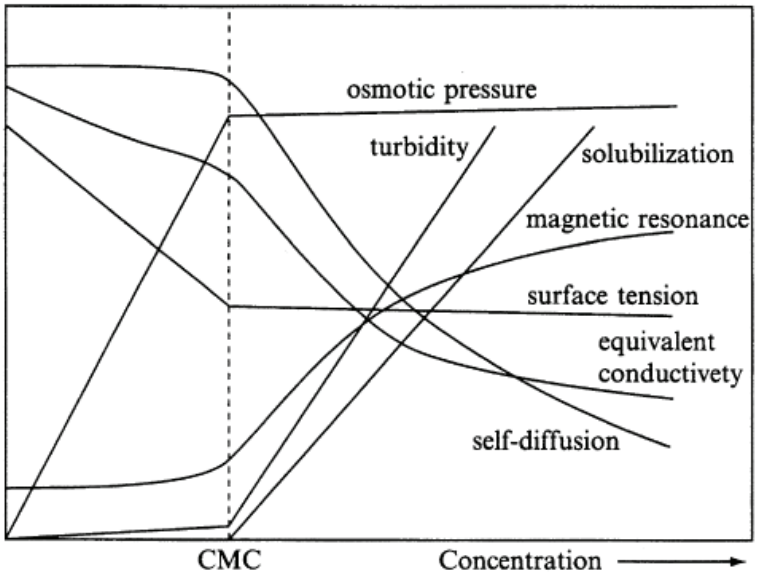

Figure 2.3. Plot showing how several properties of a surfactant solution vary with concentration. The CMC transition point is shown as a dotted vertical line.[20]

The exact configuration of the micelles and at which concentration they form is determined by the interaction between the amphiphilic molecules and the solution. The main driving force for micelle formation in aqueous solution is the hydrophobic effect caused by the

energetically unfavourable interaction between the hydrocarbon tail of the molecule and the polar solvent.[21] Factors that increase the solubility of the tail group in water, such as polar branches, decrease the influence of chain length. In addition to the hydrophobic effect the hydrophilic part of the molecule might also influence the CMC. The influence of the head group is related to two effects; first, an ionic head group increases solubility of the molecule, thereby increasing the CMC and secondly, ionic head groups leads to electrostatic repulsion between the assembling molecules, this leads to an energy barrier before micelliation in solution. In addition to the structure of the amphiphilic there are several other factors affecting the CMC. Among these are the composition of the electrolyte, the temperature and the presence of organic solvents;

- The influence of the electrolyte is seen when ionic species, like salt, are added to a solution containing ionic surfactants. The salt ions might shield the charged head group of the molecule, thus reducing the electrostatic repulsion between the charged molecules in the solution. Apart from the effect on CMC the changes in the solution chemistry might affect the micelle structure.
- A change in temperature leads to a change in the equilibrium constant for the system; this generally leads to an increase in the CMC.
- Organic solvents might affect the CMC in two ways; 1) By being included in the micelle formation as part of the micelle structure and 2) By modification of the surfactant-solution interaction. Addition of organic solvents might increase or decrease the CMC depending on the type of organic molecule that is added.

The structure of the aggregates formed when the critical micelle concentration is reached, varies greatly and might change when the concentration is increased beyond the CMC. The structure of the micelles formed also depends on the solution in which it forms. For an anionic molecule like sodium dodecyl sulphate the ionic head group will face the solution with the hydrocarbon tail forming an oil-like phase inside the micelle. In a solution of hydrocarbon (non-polar) liquid an opposite “reversed-micelle” might form where the hydrocarbon tail which is soluble in non polar liquids face the solution. The structure of the micelle is formed in such a way to minimize the total energy of the system and reduce unfavourable contact between the surfactant and the solution. An example of a micelle and a “reversed-micelle” is seen in Figure 2.4.

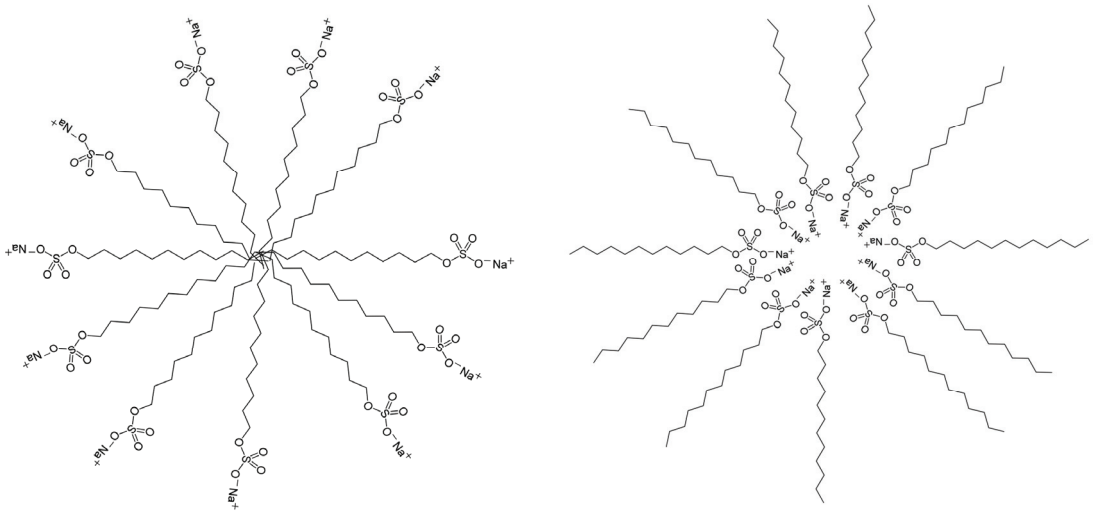

Figure 2.4. Examples of micelles formed from SDS in aqueous (left) and hydrocarbon (right) media.

The packing of surfactants into micelles and adsorbate structures have one main parameter determining the surfactant aggregate structure. This parameter is based on the size of the headgroup relative to the alkyl chan. The critical packing parameter (CPP) is thus expressed by (2.24).[22]

$$CPP = \frac{v}{lA_h} \tag{2.24}$$

where v is the volume of the carbon chain, l is the length of the carbon chain and A_h is the topological area of the headgroup. In solution, a CPP<1/3 corresponds to spherical micelles, 1/3<CPP<½ means rod-like micelles might form and ½<CPP<1 will promote formation of planar micelles.[23]

2.2.2 Surfactants adsorption on interfaces and surfaces

Self assembly of surfactants on surfaces and interfaces are caused by a combination of effects, some similar to the ones causing self assembly in solution, and is a widely studied phenomena.[24] The behaviour of the interface between two phases in a two-phase system, typically determines the fundamental properties of the system. Changes to this interface caused by the adsorption of a surfactant might therefore significantly change the

interaction between the two phases. The effect of the surfactant might vary but several key properties of the system might be affected.

- Surfactants significantly lower interfacial tensions between the involved phases.
- Surfactant adsorption might lead to the formation of electrically charged interfaces.
- Surfactant adsorption on interfaces might lead to the formation and stabilization of emulsions.
- Surfactant adsorption might lead to the formation of mechanically strong monomolecular layers at the interface.
- Surfactant adsorption might lead to a change in the hydrophobicity of solid surfaces.

There are a number of mechanisms by which surfactants might adsorb onto interfaces. Corrosion inhibitors are designed to adsorb onto the solid-liquid interface and adsorption onto solids will therefore be the main focus of the discussion. In general the adsorption involves single ionic species and not the adsorption of micelles.[25] Below is a short summary of the main adsorption mechanisms.[26,27]

- Ion exchange: Replacement of ions attached to a surface by similarly charged surfactant ions (covalent bonding).
- Ion pairing: Adsorption of surfactant on unoccupied charged surface of opposite charge (electrostatic attraction).
- Hydrophobic bonding: Adsorption of surfactants due to the interaction between hydrophobic groups on the surface and the hydrophobic part of the surfactant.
- Polarization of π electrons: Electron rich groups on the surfactant interact with positive sites on the surface. Attraction forces leads to adsorption.
- Adsorption by dispersion forces: London-van der Waals forces between adsorbate and adsorbent, increasing force as the molecular weight of the adsorbate increases. This includes lateral associative interaction between groups in the hydrocarbon chain of the surfactant.

The driving force for adsorption on solids is thus a combination of electrostatic and hydrophobic forces, rather than purely hydrophobic as for the micelle formation in solutions. From the standard free energy of adsorption an expression for the adsorption density on the Stern plane (inner Helmholtz plane) (Γ_s) has been proposed:[28]

$$\Gamma_s = lc_b \exp\left(\frac{-\Delta G^0_{ads}}{RT}\right) \tag{2.25}$$

Where l is the effective length of the hydrocarbon chain, c_b is the bulk concentration, R is the gas constant, T is temperature in Kelvin and $-\Delta G^0_{ads}$ is the standard energy of adsorption. The standard driving force for adsorption is the sum of a number of forces:

$$-\Delta\overline{G^0_{ads}} = \Delta G^0_{elec} + \Delta G^0_{chem} + \Delta G^0_{c-c} + \Delta G^0_{c-s} + \Delta G^0_H + \Delta G^0_{H_2O} + ... \tag{2.26}$$

where ΔG^0_{elec} is the free energy contribution from electrostatic interactions, ΔG^0_{chem} is from covalent bonding, ΔG^0_{c-c} is from lateral associative interaction, ΔG^0_{c-s} is from hydrophobic interaction, ΔG^0_H is from hydrogen bonding and $\Delta G^0_{H_2O}$ is from the salvation of adsorbate species. There are several intermolecular forces that can be included in the considerations on electrostatic forces such as ion-ion repulsion, ion-dipole repulsion and dipole-dipole interactions. All of these forces are important in surfactant chemistry due to the nature of water molecules.

The forces acting against adsorption are also of interest. Of these forces electrostatic repulsion based on a net charge on a molecule is the strongest and has a longer range than all the other multipole interactions.[18] As a result, this force is typically the most important force in systems with an electrolyte or charged surface. As explained in chapter 1.1 a surface in contact with an electrolyte develops a double layer consisting of the solution constituents. This double layer structure has a distribution of charge in which electrostatic repulsion of charged surfactants might occur. The double layer formation is also greatly affected by the state of the surface which typically develops a surface charge when exposed to an electrolyte. This might be cased by effects such as preferential dissolution in

the solids lattice (clays), ionization of surface groups (silica) or electrochemical reactions involving the surface atoms (corroding iron).

The adsorption of ionic surfactants such as corrosion inhibitors on charged surfaces might therefore be enhanced or decreased depending on the charge of the surface. However, the effect of surface charge varies depending on the electrolyte. Effects such as shielding of charge due to solvent ions decrease the effect of the electrostatic repulsion and are thus a main factor in surfactant adsorption. Solid surfaces in aqueous environments exhibit different affinities to the water molecules. This water affinity is what determines the wetting behaviour of the surface and is important to the adsorption and interaction between the solution and the surface. Surfaces with a high affinity for water are called hydrophilic surfaces; typical examples are mineral oxides and silica which might form hydrogen bonds with the water through the surfaces functional groups. Surfaces with a low affinity for water are, on the other hand, called hydrophobic surfaces. These surfaces typically exhibit hydrocarbon properties.

2.2.3 Surface excess

Adsorption onto surfaces or interfaces differs from the pure solution chemistry in that the interactions between the surface and the surfactants might lead to the accumulation of surfactants on the surfaces exceeding the concentration found in solution; this is referred to as the surface excess. The surface excess of a system is related to the changes in properties of the interface and is an important thermodynamic concept when dealing with surfaces. The concept was introduced by Gibbs who developed a relation between the chemical potential of the substances present at a surface and the changes in surface tension. Gibbs looked at two phases, α and β, and the interface between the two. The interface can be viewed as a transition area with a thickness Δx which can be treated as a phase of its own, σ_p. This interface has properties different from the properties of the two adjacent solutions. Gibbs then defined an imaginary surface (X_0) which divides the phases so that an evaluation of the surface excess at this plane is possible. The difference between the imaginary concentration of species *i* and the real concentration (the hatched region in Figure 2.5) was then defined as the surface excess.

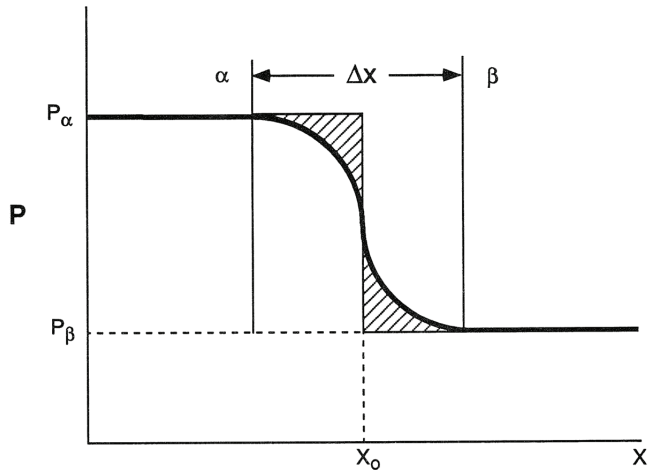

Figure 2.5. Sketch showing the imagined interface used as the basis for the determination of the Gibbs surface excess.[18]

Gibbs definition of the surface excess per area (Γ_i) is:

$$\Gamma_i = \frac{n_i^\sigma}{A} \tag{2.27}$$

where n_i^σ is the surface excess in moles.

By combining equations for changes in energy for two adjacent phases and the interface an expression for the change in energy brought about by changes in T, p or n_i can be found. [18] The energy (En^i) for a system consisting of the three phases α, β and σ are given by (2.28):

$$En^{tot} = En^\alpha + En^\beta + En^\sigma \tag{2.28}$$

The energy of the interface can then be described in a similar way to the energy of a bulk phase so that the differential of the surface internal energy is:[18]

$$dEn^\sigma = TdS^\sigma + \gamma dA + \sum_i \mu_i^\sigma (T, n_i^\sigma) dn_i^\sigma \tag{2.29}$$

where the work term pdV (for a bulk phase) has been replaced by a surface expression of γdA, where γ is the surface tension. If the energy (E^σ), entropy (S^σ) and moles (n_i^σ) at the

interface are increased from zero to a given value the energy of the interface can be written as:[18]

$$En^{\sigma} = TS^{\sigma} + \gamma A + \sum \mu_i n_i^{\sigma} \tag{2.30}$$

If equation (2.30) is differentiated and compared to equation (2.29) we get the Gibbs adsorption equation:

$$S^{\sigma} dT + A d\gamma + \sum n_i^{\sigma} d\mu_i = 0 \tag{2.31}$$

At a constant temperature this yields the Gibbs adsorption isotherm:

$$d\gamma = -\sum_i \Gamma_i d\mu_i \tag{2.32}$$

This equation can then be used to determine surface excess of components at a surface by making measurements of surface tension and careful placement of the imaginary Gibbs surface. A typical approach for a two component system is to locate the surface so that the surface excess of one of the components is zero.

2.2.4 Adsorption isotherms

In surface science it is often desirable to determine the amount of adsorbed surfactant per unit area or mass. A plot of the adsorbed species per unit area versus concentration can then be made; this plot is called an adsorption isotherm. Thus, this is a measure of the coverage of the surface by surfactant at a given condition. A number of studies on both cationic and anionic surfactants have been conducted on solid surfaces.[26,29-32]

For simple solutions the adsorption behaviour of a molecule can be modelled through the development of an adsorption isotherm. The various adsorption isotherms used are based on different sets of assumptions regarding the adsorbate. A thorough understanding of the system that is to be tested is therefore necessary. In its simplest form this adsorption can be modelled up to one monolayer coverage by the Langmuir Isotherm (2.33).

$$\Gamma = \Gamma_m \left(\frac{Kc_b}{1 + Kc_b} \right) \tag{2.33}$$

Where Γ is the surface excess and Γ_m is the surface excess for a dense monolayer. c_b is the bulk concentration and K is an equilibrium constant. The Langmuir isotherm is based on four assumptions; 1) The surface is homogenous 2) The surfactant adsorbs in only one monolayer 3) There are no surfactant-surfactant or surfactant-solvent interactions 4) The surfactant an solvent molecules have equal cross-sectional surface areas. In general only the first two of these assumptions are reasonably true. Several models that have been developed for systems where the surface coverage leads to interaction between the adsorbents, attempt to account for this interaction. Adsorption isotherms expressed on a linear scale typically display two plateau regions and one steep increase.[33] Figure 2.6 shows the adsorption isotherm in the simplest form with two plateau regions.

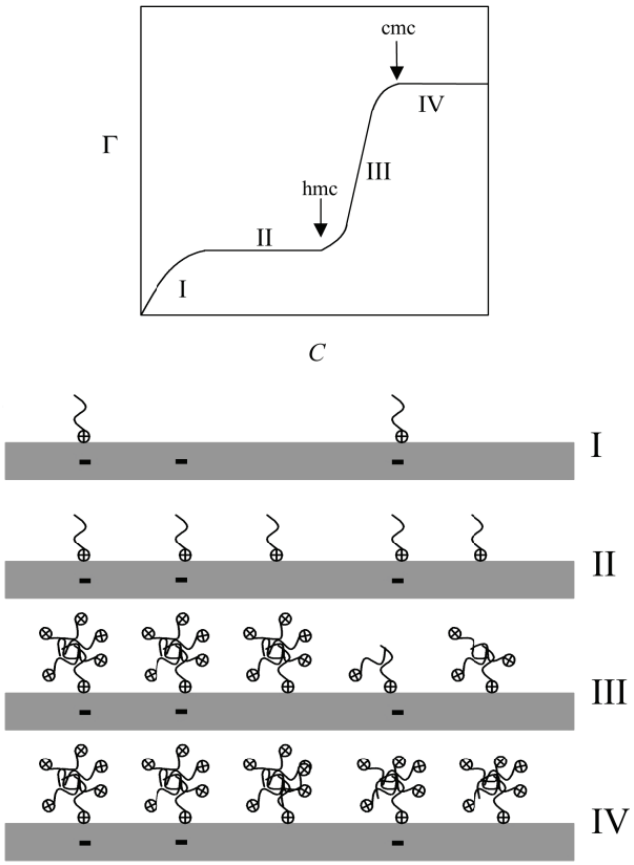

Figure 2.6. Sketch showing the adsorption isotherm in the simplest form with two plateau regions and a possible development of the surface adsorbent structure.[34]

Gao et al. suggested different mechanisms governing the four regions of the adsorption isotherm.[34] In region (I) the surfactant adsorbs via electrical interactions with the surface, the surface excess is at this level mainly determined by the surface charge. No interaction between the surfactant molecules. In region (II) the surface charge has been neutralized but still only monomers adsorb with no interaction. In region (III) the onset of surfactant–surfactant hydrophobic tale-interactions occur. This leads to an abrupt increase in the amount of adsorbed surfactant and the formation of hemicelles.[34] Region (IV) starts at the point where the CMC for the surfactant is reached and further increasing the concentration does not lead to a further increase of the surface excess. This three region adsorption model accounts for many of the simple adsorption processes occurring but is not the only model developed. Figure 2.7 shows the four region model developed by Somasundaran and Fuerstenau for adsorption with a reversed surfactant orientation.[35] In this model the initial

adsorption is similar to what was proposed by Gao et al. In region (II), however, the onset of strong lateral interaction and aggregation is proposed as a possible mechanism. The surfactants forms islands where the tail of the molecules face the solution and these patches might therefore exhibit hydrophobic properties. This type of behaviour has been confirmed by various surface techniques such as contact angle measurements, and Raman spectroscopy.[35,36] Region (III) has an increase in surface excess due to growth of the aggregates formed in region (II). When a complete bilayer has formed the adsorption reaches a plateau, region (IV), and no further increase in surface excess is seen. The main difference between the two-step and the three-step models are thus the hydrophobic interactions between the tail groups which are accounted for in the three-step model.

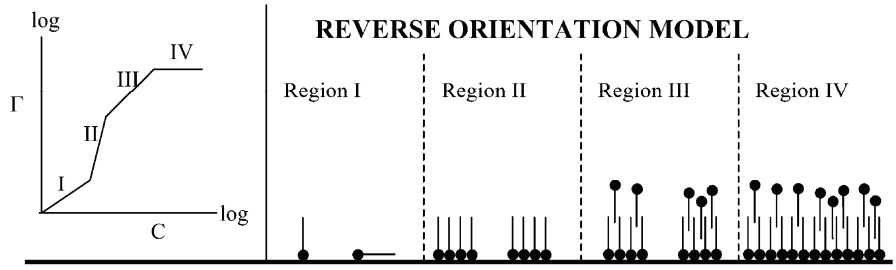

Figure 2.7. The figure shows how Somasundaran and Fuerstenau envisioned the development of the surface excess when lateral interactions are accounted for.[31]

The adsorption models are typically used to describe the effect of change in solution and the differences between various surfactants. Studies of change in carbon chain length and head group-surface interaction can also be done by plotting solution depletion curves. One significant limitation with the model is the use of surface charge as an adsorption parameter. Goloub et al. published data showing that both pH and adsorption of the surfactant greatly affects the surface charge of the substrate.[37] Since the pH might cause the ionization of surface groups the pH might change along one isotherm, thus changing the conditions for adsorption depending on the concentration of adsorbent. In addition to this effect the realization that the electrolyte concentrations also greatly affects the adsorption has lead to the development of methods for detecting charge neutralization points (or the isoelectric point) based on surfactant measurements with several concentrations of electrolyte.[37] The driving force for adsorption can, based on these

findings, be divided into two regions: 1) adsorption due to electrostatic interactions between the headgroup below the IEP and 2) adsorption due to hydrophobic interaction between the monomers where charge neutralization has been realized.

2.3 Particles as surfactants

The connection between the wetting of a particle, which in surface chemistry refers to the extent of contact established between a liquid and a solid surface when the two are brought together, and the effect a particle has on emulsions was first commented on by Pickering around 1900.[38] His initial study of oil in water has later been expanded and a better understanding of the phenomena has been achieved.[39,40] The understanding of emulsions stabilized by fines has also been an increasing field of interest in the oil industry where water-in-oil emulsions are creating corrosion problems.[41]

Surfactants can be characterized by the hydrophile-lipophile balance (HLB) of the molecule.[42] This balance then describes the water/oil preference of the molecule and thus the effect it may have on the interface between two phases. Similar to this characterization a particle can be described in terms of its wettability via contact angle.[43] There are however some major differences between surfactant molecules and particles.

- Particles do not assemble to give aggregates in the same way surfactant molecules form micelles (solubility phenomena are absent).
- The contact angle is the parameter governing the tendency of a particle to move into the oil or the water phase. For amphiphilic molecules, the HLB is the determining factor.
- At liquid/liquid interfaces particles are mainly irreversibly adsorbed while surfactant molecules adsorb and desorb at a relatively fast timescale.

The behaviour of small particles in an oil/water system can be divided into three groups based on the particles wetting properties. If the degree of wetting is determined by contact angle, hydrophobic particles will, in an aqueous/oil system, yield contact angles >>90º. In such a case the main fraction of the particle resides in the non polar liquid phase (oil). If the contact angle is <<90º (hydrophilic particle) the main fraction of the particle resides in

the polar liquid (water). The third situation arises when the contact angle is around 90º. This means that the particle surface has a comparable affinity to both the oil and the water and the particles will in this situation aggregate at the interface. Due to the difference in size of the wetted fraction of the particles the interface between the oil and water will form a curved interface such that the larger part of the particle resides on the external side of the curvature. An example showing this effect is shown in Figure 2.8.

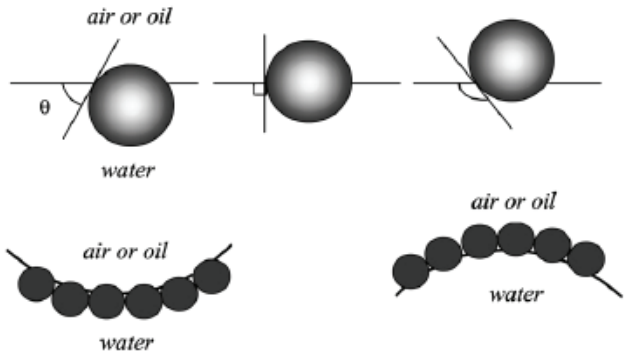

Figure 2.8. The figure shows how the hydrophobicity (from slightly hydrophilic to slightly hydrophobic) of a particle determines the curvature of the interface.[42]

The adsorption of particles on an interface differs greatly from that of a surfactant molecule. The main difference is that for particles the adsorption energy is a key parameter in the particle-interface interaction. To understand this interaction several factors must be considered. A particle in phase A adsorbing on a phase boundary A-B must exchange a part of the phase boundary of A-B with a system where the particle is partially wetted by the two phases. The energy of the A-B phase boundary is normally quite large and the adsorption usually leads to a significant drop in total energy involved. This makes the energy of adsorption large. The maximum energy of adsorption is achieved for a particle with a contact angle of 90º, at either side of this value the energy of adsorption rapidly drops down to lower values. This adsorption effect can be quantified by an equation describing the energy required (*En*) to remove a particle from the interface A-B.

$$En = \pi r^2 \gamma_{AB} \left(1 \pm \cos\theta\right)^2 \tag{2.34}$$

Where γ_{AB} is the interfacial energy between the phases A and B. This thermodynamic evaluation of the interfacial adsorption also concludes that the maximum in emulsion stabilization tendency for particles is seen for contact angles around 90 º. The effectiveness of the solid particle in stabilizing emulsions depends on several factors.

- Particle size
- Particle shape
- Concentration
- Particle wettability
- The interaction between particles
- The media in which the solids are suspended prior to emulsification

There are two main mechanisms by which colloidal particles stabilize emulsions:

1. Particles adsorb at the oil-water interface and remain there forming a dense film around the dispersed spheres impeding coalescence. A steric barrier thus prevents the droplets from coalescing.
2. Additional stabilization arises when the particle-particle interactions are such that a three dimensional network of particles develops in the continuous phase surrounding the drops.

In systems stabilized by the second mechanism, increased viscosity is seen. Extremely stable emulsions have been seen when this type of stabilization is involved. In addition to the emulsification tendencies seen with particles the particles might aggregate heavily at interfaces without creating emulsions. Both mechanisms might lead to severe problems in oil and gas transport and separation processes.

3 CO_2 corrosion

Corrosion may be defined as a degradation of a material caused by an environment. There are thus a multitude of environments and materials that may be subjected to corrosion. Perhaps the most widely studied environment that may cause corrosion of metals is the aqueous system. Corrosion of metals in an aqueous environment typically involves the reduction of oxygen present in the solution and involves electrochemical reactions where both transfer of charge and changes in chemical state of the involved species occur. When oxygen is not present other species might take over as the main corrosive component in the aqueous solution. Dissolved CO_2, which forms carbonic acid, is one such component. In systems containing CO_2 gas, the carbonic acid created by the CO_2 contributes significantly to the corrosion of the metal surface. In environments free of oxygen the dissolved CO_2 might completely govern the corrosivity of the system.

3.1 Corrosion basics

To understand CO_2 corrosion, it is necessary to have a basic knowledge regarding the charge transfer reactions involved in corrosion. The simplest charge transfer reaction is the oxidation of a metal atom, *i* (ex. $Zn = Zn^{2+} + 2e^{-}$). The energy involved in such an oxidation is governed by changes in Gibbs energy (ΔG). The *Nernst equation* (3.1) describes this basic relationship between a single charge transfer reaction and the energy involved:

$$E_{i^+/i}^{rev} = E_{i^+/i}^{0} - \frac{RT}{nF}\ln(Q) \tag{3.1}$$

and

$$\Delta G = -nFE_{i^+/i}^{rev} \tag{3.2}$$

where $E_{i^+/i}^{rev}$ is the reversible cell potential for a reaction where *i* is oxidised. *Q* is the product of the activities of reaction products divided by the product of activities of the reactants. $E_{i^+/i}^{0}$ is the standard cell potential at equilibrium ($E_{i^+/i}^{rev} = 0$, *Q=equilibrium const.*).

When a metal corrodes both oxidation and reduction reactions occur simultaneously at the metal surface. The cell potential is thus a product of both the oxidation and reduction reactions. The mixed potential theory describes how no electrical charge can accumulate during a corrosion reaction.[44] This means that the energy of the system depends on both oxidation and reduction reactions. In order to determine how the current and potential of mixed potential systems behaves the overpotential (η) is introduced. The overpotential for a single electrochemical reaction is defined as:

$$\eta = E - E^{rev} \tag{3.3}$$

In a mixed potential system the corrosion potential (E_{corr}) may replace the reversible potential (E^{rev}) in equation (3.3). The overpotential in corrosion science is therefore calculated based on E_{corr} rather than E^{rev}. An expression for the net current in the system, found from the Gibbs energy involved in an electrochemical reaction, is given in equation (3.4).[45] The total current is then the sum of the anodic and cathodic part currents. The equation describes the relationship between the actual rate of the reactions and the potential of the cell. This expression is called the *Butler-Volmer equation*. Assuming no mass transfer effects the equation is given by (3.4):

$$i = i_a - |i_c| = i_0 \left[\exp\left(\frac{(1-\alpha) zF\eta}{RT} \right) - \exp\left(\frac{-\alpha zF\eta}{RT} \right) \right] \tag{3.4}$$

where α is the charge transfer coefficient for the reaction and i is the current. i_0 is the exchange current and is the balanced faradaic activity occurring when the net flow of current is zero. The letters c and a are the cathodic and anodic part currents respectively. The above equation describes the current responses to a change in potential for an activation controlled system. The Butler-Volmer equation has two limiting cases: high positive and high negative overpotential. At these two extremes the equation can be reduced to two simple expressions for anodic (equation 3.5) and cathodic (equation 3.6) overpotentials based on the current.

$$\eta_a = \frac{RT}{(1-\alpha)zF}\log\left(\frac{|i|}{i_0}\right) \tag{3.5}$$

$$\eta_c = -\frac{RT}{\alpha zF}\log\left(\frac{|i|}{i_0}\right) \tag{3.6}$$

These two expressions can then be generalized in the *Tafel equation* (3.7).

$$\eta = a + b\log|i| \tag{3.7}$$

a and *b* are constants. The Tafel equation is an analytical expression which can be used to evaluate $E - \log|i|$ curves for overpotentials far from equilibrium. A plot of $E - \log|i|$ is one of the most common ways to represent electrochemical data including corrosion processes. An example of this type of plot is seen in Figure 3.1. As seen from the Tafel equation the $E - \log|i|$ plot has an angle b (Tafel slope). The Tafel slope is a function of the reaction rate which is normally different for the anodic part reaction (b_a) and for the cathodic part reaction (b_c). At high positive and negative overpotentials the slope is normally linear. Concentration terms will also affect the Tafel curves (move away from linearity) but only at very high overpotentials ($\eta = E - E_{corr}$). The kinetics of the anodic and cathodic part reactions can then be determined by the slope of the part currents. By extrapolation of the tangents for the anodic and cathodic part reactions the value of the corrosion potential E_{corr} and the corrosion current i_{corr} for the system can also be found. Both values are found at the point where the tangents cross. The potential in these types of experiments is measured against a reference electrode. The exact values of the potentials reported might therefore vary.

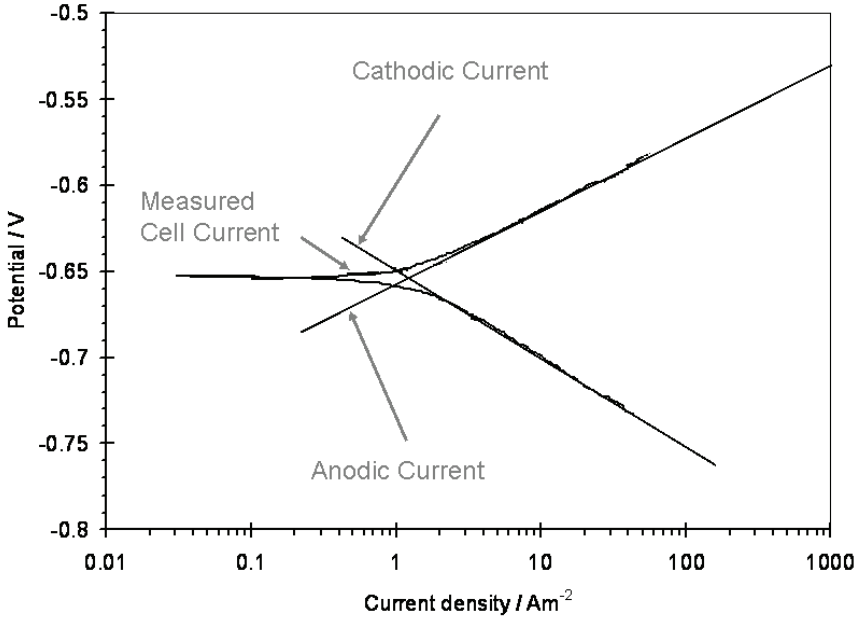

Figure 3.1. Graph showing the linearity of the part currents in an $E - \log|i|$ *experiment. The influence of mass transfer is not taken into account.*

In addition to the limits of high positive and high negative overpotentials on the Butler-Volmer equation the equation can be simplified when the overpotential is very small. By using the Taylor expansion series on the exponential functions in (3.4) it reduces to:

$$i = i_0 \frac{nF\eta}{RT} \tag{3.8}$$

The ratio $-\frac{\eta}{i}$ has units of resistance and can be defined as the charge transfer resistance (R_{ct}) of the system. A linear relationship for the current-resistance is then found for small overpotentials (3.9).

$$R_{ct} = \frac{RT}{nFi_0} \tag{3.9}$$

3.2 Corrosion in the presence of CO_2

Carbon dioxide (CO_2) gas in aqueous solutions dissolves and reacts to form corrosive components. The activity (a_i) of a solute gas in a liquid is proportional to the partial pressure of that gas above the solution. For simplicity the activity of the solute gas is replaced by the concentration (c_i). Henry's Law (3.10) describes the relationship between partial pressure of a gas and the equilibrium concentration in the aqueous phase for real solutions at low concentrations:

$$p = K_{H,i(T)} c_i \tag{3.10}$$

Where p is the partial pressure $K_{H,i}$ is Henry's constant at the relevant temperature and c_i is the molar concentration.[11] The CO_2 gas dissolved in the water then hydrates to form a weak acid by the following reaction:

$$CO_2 + H_2O \leftrightarrow H_2CO_3 \tag{3.11}$$

Only a small amount of the dissolved carbon dioxide will hydrate to form carbonic acid (~0.26 %).[46] The weak acid then dissociates in two steps:

$K_{sol,\,1}$ $$H_2CO_3 \leftrightarrow H^+ + HCO_3^- \tag{3.12}$$

$K_{sol,\,2}$ $$HCO_3^- \leftrightarrow H^+ + CO_3^{2-} \tag{3.13}$$

This dissociated acid renders the system more corrosive than what the pH would suggest for a pure aqueous oxygen free system. The impact of CO_2 on the corrosivity of an aqueous system has been described by Nesic et al.[47] A series of experiments using electrochemical sweep techniques in different pH regions clearly demonstrated that different reaction mechanisms are present in a system containing CO_2, compared to a system where the reduction of protons is the dominating cathodic reaction. Figure 3.2 shows how two systems where one contains CO_2 behaves at pH 4. It is clear that the introduction of CO_2 increases the corrosion rate but no change in Tafel behaviour for the cathodic reaction is seen. The relative increase in corrosion rate can probably be attributed to direct reduction of H_2CO_3.[48]

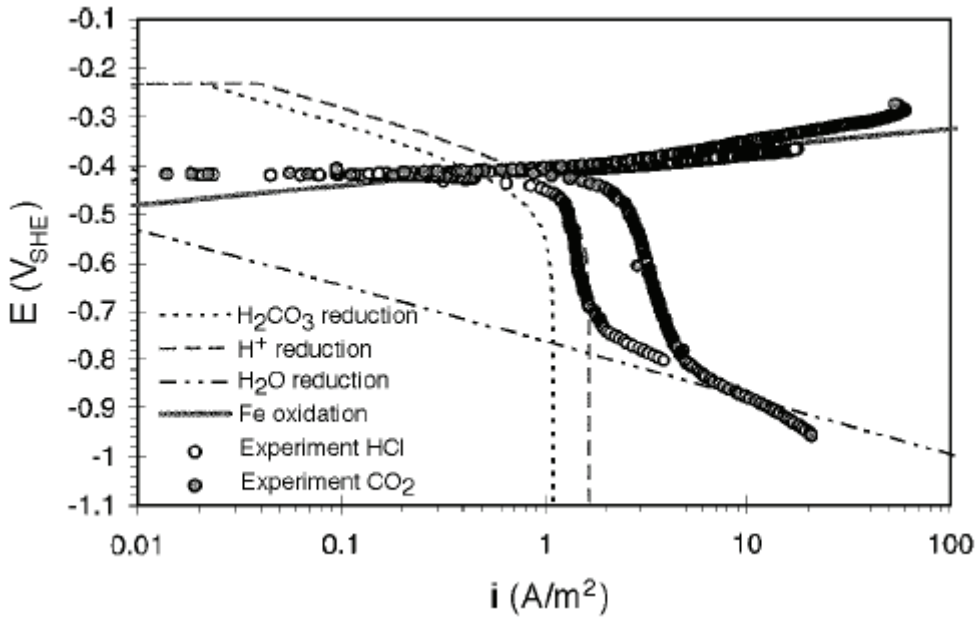

Figure 3.2. Effect of CO_2 on the corrosion rate in brine at pH 4, 3% NaCl, 1 bar, T=20℃.[47]

When the pH is increased to 5, it becomes apparent that the impact of CO_2 is even greater at higher pH levels. The effect of proton reduction compared to direct reduction of H_2CO_3 is negligible. This can be seen in Figure 3.3 where the Tafel slope for proton reduction approached that of direct reduction of water.

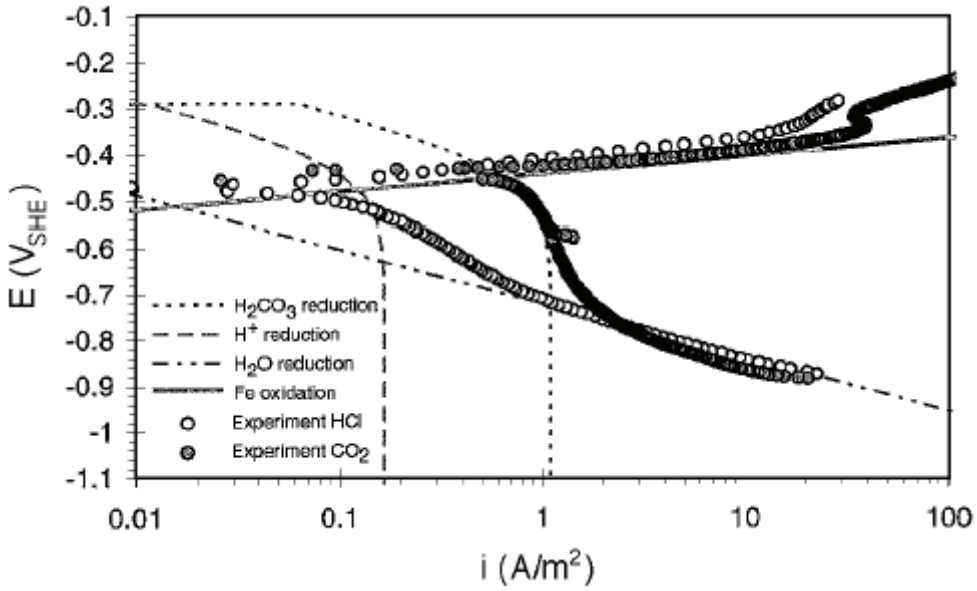

Figure 3.3. Effect of CO_2 on the corrosion rate in brine at pH 5, 3% NaCl, 1 bar, T=20 °C.[47]

There are several possible cathodic and anodic reactions in the CO_2 corrosion system, and several papers have been published discussing this.[47-50] De Waard and Milliams proposed one of the first corrosion mechanisms for corrosion of steel in CO_2 solutions. The reaction mechanisms included direct reduction of carbonic acid as the dominant cathodic mechanism.[48] Direct reduction of H_2CO_3 means that no dissociation of the carbonic acid has taken place prior to the reduction reaction.

$$H_2CO_3 + e^- \rightarrow \frac{1}{2}H_2 + HCO_3^- \tag{3.14}$$

This reduction step is, however, not thought to be the rate-determining step leading to the limit current density seen in the figures above. The hydration of CO_2, which is a pure chemical reaction, is a much slower process and is thus usually the rate-determining step for the reaction.[50] The reduction of the somewhat less abundant bicarbonate (HCO_3^-) is also possible but the contribution to the overall current density from this step is thought to be small.

$$HCO_3^- \rightarrow \frac{1}{2}H_2 + CO_3^{2-} \tag{3.15}$$

If the potential lies above the point where the dominant reaction has changed to the direct reduction of water, the resulting current is not limited by reactants transport.

$$H_2O + e^- \rightarrow H + OH^- \tag{3.16}$$

The anodic reaction mechanism for CO_2 corrosion was proposed by Bockris *et al.*[49] He proposed a reaction mechanism involving OH^- as part of the reaction route. It is probably correct at high pH (pH>5) values, but a more complex system is found for lower pH values due to the presence of other ligands, than what was found in the mechanism suggested by Bockris et al.[47] The simple steps proposed were:

$$Fe + OH^- \rightarrow FeOH + e^- \tag{3.17}$$

$$FeOH \overset{RD}{\rightarrow} FeOH^+ + e^- \tag{3.18}$$

$$FeOH^+ \rightarrow Fe^{2+} + OH^- \tag{3.19}$$

As these steps show the overall reaction leads to the release of electrons and the dissolution of iron ions. Recent studies have uncovered possible errors in the assumptions leading to the corrosion model devised by de Waard and Milliams and the one proposed by Bockris et al.[51,52] A more complex corrosion system for the CO_2 model has therefore been proposed. In a comprehensive paper by Nesic et al.[47], several corrosion mechanisms were proposed based on the pH of the system. Distinct anodic mechanisms were observed for pH<4 and pH>5, while a transition from one mechanism to the other was proposed for the intermediate area. This means that different b_a-values for the anodic part reactions should be used when calculating corrosion rates, depending on the pH of the system.

3.2.1 The effect of CO_2 partial pressure on CO_2 corrosion mechanisms

As discussed, the pH affects the intermediate steps involved in the anodic and cathodic part-reactions in the CO_2 corrosion system. The effect of CO_2 partial pressure on the cathodic Tafel slopes is also significant. An increase in CO_2 partial pressure at a stable pH does not lead to a change in the reaction mechanisms but rather an increased current in the anodic sweep. This effect can be related to the surface coverage of the CO_2 on the surface of the steel. Since the dissolution mechanism for iron in CO_2 corrosion involves CO_2 as part of a ligand the availability of CO_2 on the surface is important. The transition between no surface coverage to full surface coverage can than be used to explain the increased corrosion current in Figure 3.4.[47]

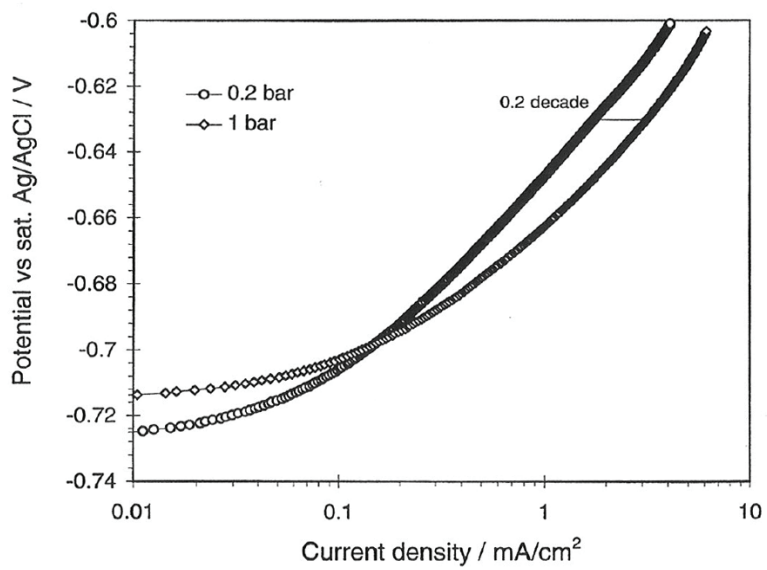

Figure 3.4. Effect of CO_2 partial pressure on anodic potentiodynamic sweeps for a steel electrode at pH 6.[47]

The increase in current with CO_2 partial pressure is limited both at the low and high ends. For $pCO_2 < 0.1$ bar no significant effect on the current is seen. When the partial pressure increases to 0.1 bar $< pCO_2 <$ 1 bar an increasing, linear, effect of CO_2 on the current is seen. At partial pressures above 1 bar CO_2 no further effect of the increased partial pressure was seen.[47] The effect of bulk and surface diffusion effects as a function of CO_2 partial pressure were not considered in this study. Increasing the CO_2 pressure increases the concentration of carbonic acid in solution, as seen in equations 3.10 and 3.11. An

increased pressure will therefore affect any corrosion limiting reactions that are diffusion limited.

3.3 Formation of iron carbonate

When the carbon steel corrodes, Fe^{2+} is released into the electrolyte as a corrosion product. In an oxygen free CO_2 corrosion environment this free iron might then react with the carbonate in the system to form iron carbonate.

$$Fe^{2+} + CO_3^{2-} \rightarrow FeCO_3 \tag{3.20}$$

$$Fe^{2+} + HCO_3^{-} \rightarrow FeCO_3 + H^{+} \tag{3.21}$$

The solubility limit for iron carbonate must be exceeded near the steel surface for the iron carbonate to form and remain stable. As the two reactions above clearly demonstrate the amount of free iron and bicarbonate in the system is ultimately what determines if an iron carbonate phase will precipitate. The exact amounts of free iron and carbonate in an equilibrium system might be calculated using the solubility products for the system. For iron carbonate we have:

$$K_{sp} = \left[Fe^{2+}\right] \times \left[CO_3^{2-}\right] \tag{3.22}$$

For carbonic acid we then get:

$$K_{sol,1} = \frac{\left[H_2CO_3\right]}{p_{CO_2}} \tag{3.23}$$

$$K_{sol,2} = \frac{\left[HCO_3^{-}\right] \times \left[H^{+}\right]}{\left[H_2CO_3\right]} \tag{3.24}$$

$$K_{sol,3} = \frac{\left[CO_3^{2-}\right] \times \left[H^+\right]}{\left[HCO_3^-\right]} \tag{3.25}$$

If $K_{sol,3} << K_{sol,2}$, the pH (or H^+ concentration) can be calculated from equation (3.23) and (3.24) only.[53] The pH can thus be directly related to the pressure of CO_2 and the solubility of $FeCO_3$.

$$\left[H^+\right] = \frac{K_{sol,1} K_{sol,2} p_{CO_2}}{\left[HCO_3^-\right]} \tag{3.26}$$

If the equations (3.22) to (3.26) are combined an expression for the ferrous ion concentration can be found:

$$\left[Fe^{2+}\right] = \frac{K_{sp}}{\left[CO_3^{2-}\right]} = \frac{K_{sp} \times \left[H^+\right]^2}{K_{sol,1} K_{sol,2} K_{sol,3} p_{CO_2}} \tag{3.27}$$

As these considerations show, the formation of iron carbonate is fairly complex with several species affecting the formation, among which the pH and the ratio of Fe^{2+} to the partial pressure of CO_2 are the most significant. In practice the solubility product must be much higher than predicted from these considerations. This means that the Fe^{2+} level increases beyond the level found from (3.27) before precipitation initiates. The reason for this might be the formation of complexes that interfere with the formation of the corrosion film. This means that the rate of formation of corrosion product must overcome the dissolution before the growth of a $FeCO_3$ layer will initiate.

The above considerations also demonstrate the significant effect of pH on the formation of iron carbonate. A second order dependence is found for pH. This effect is clearly demonstrated by Dugstad et al. who found that the reduction in solubility is especially high when the pH increases beyond 5.[54] This is shown in Figure 3.5 where the solubility of iron carbonate is shown in water at 60 °C with a partial CO_2 pressure of 1 bar.

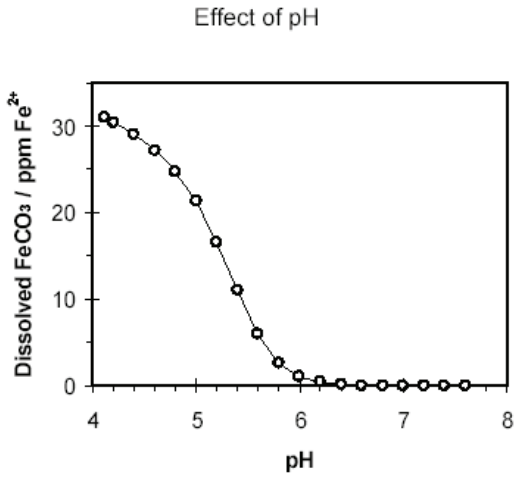

Figure 3.5. The plot shows how solubility of $FeCO_3$ changes as a function of pH. The CO_2 pressure is 1 bar at 60 ºC.[55]

3.4 Corrosion mitigation

Several different approaches in mitigation of CO_2 corrosion of carbon steel have been developed, depending on the fluid condition and chemistry of the fluids in the system. The use of corrosion inhibitors and the manipulation of surface deposits are two possible ways of lowering the corrosion rate.[2,3] Corrosion inhibitors are typically used in aggressive environments or pipelines where formation water (high levels of scale forming ions like Ca^{2+} and Mg^{2+}) is present in the fluid flow. Techniques involving preferential precipitation of iron carbonate on the steel surface are typically used in pipelines transporting gas condensate.

3.4.1 Corrosion inhibitors

Corrosion inhibitors are a class of organic molecules specifically designed to mitigate corrosion of metals. The national association of corrosion engineers (NACE) defines corrosion inhibitors in the following way: A substance which retards corrosion when added to an environment in small concentrations.[56] Several papers have been published regarding adsorption and inhibition by long chained hydrocarbons.[3,5,7,57,58] CO_2 corrosion inhibitors typically consist of amphiphilic, surface-active molecules with hydrocarbon chains typically in the range C12-C18. The effectiveness of corrosion inhibitors are affected by

the condition under which it is applied and the surface-inhibitor interaction. The inhibition is thought to be caused by a combination of the following effects;

- Dense inhibitor layers may reduce the area available for reactions and reduce mass transfer near the surface.
- Adsorption on active anodic sites on the surface changes the activation energies involved in the dissolution of the metal surface, thereby lowering corrosion rate.
- The corrosion potential changes due to adsorption of inhibitor, affecting the point at which the cathodic polarisation curve changes from activation controlled to mass transfer control.[59,60]

Adsorption can be divides into two types; physical adsorption (physisorption) and chemical adsorption. The interacting forces involved in physisorption are weak intermolecular forces (van der Waals forces). Attraction is in this adsorption type caused by mutual changes in the dipole moment of the involved species. Inhibitor compounds are generally ionic in nature and the adsorption is thus not a typically a physisorption type adsorption. Chemical adsorption (chemisorption) occurs when the forces involved are valence forces (the same kind as the forces involved in the formation of chemical compounds). The adsorbed species and the surface forms a coordinate-type bond (covalent or ionic), due to the transfer or sharing of the inhibitor molecules charge (electrons). For corrosion inhibitors adsorption is caused by a combination of two main effects; 1) the molecules in solution are pushed out of the polar water due to the hydrophobic effect and 2) the inhibitor molecules adsorbs on the surface through a chemical adsorption step. After the inhibitor is adsorbed on the surface it may take some time to reach equilibrium adsorption and desorption for the inhibitor on the steel surface. This time to reach equilibrium is detected as a delay in the inhibitor performance.[60,61] The effectiveness of the inhibitor to adsorb and form chemical bonds to the surface metal is probably what determines the inhibitors efficiency.[62] In general, the electron density of the donor atom on the functional group and the polarizabillity of the group determine the strength and efficiency of the bond formation. For typical inhibitor compounds such as imidazolines a bond formation due to the ρ-π conjugation which is present in the N-C-N bond in the imidazoline molecule head group enables a strong bonding to the surface. This conjugation in particular enables the formation of a strong bond between the nitrogen atom and the

metal substrate since the conjugation readily accepts the introduction of releasing constituent on the carbon atom.[59] Sastri suggested the following ordering of donor atoms in functional groups based on polarizability and electronegativity of the elements; Se > S > N > O.[62]

Several electrochemical techniques have been developed to investigate the effect of corrosion inhibitors on the corrosion processes of steel. The use of potential sweep techniques and electrochemical impedance spectroscopy measurements have previously been performed to investigate the effects the inhibitors might have on the corrosion processes of steel. In impedance measurements a large change in charge transfer resistance is typically measured when efficient inhibitors are added to the solution. In polarization resistance (PR) measurements a shift to higher potentials and lower corrosion rates in the E-log|i| plot is usually observed following inhibitor addition. Examples showing the changes related to the inhibitor addition are seen in Figures 3.6 and 3.7. Figure 3.6 shows how the modulus of the impedance increases in the low frequency area when the corrosion inhibitor is added. This indicates that the inhibitor influences the charge transfer processes at the steel surface. In Figure 3.7 it can be seen that both the corrosion potential (E_{corr}) and the corrosion rate plotted in the E-log|i| diagram changes significantly following inhibitor addition.

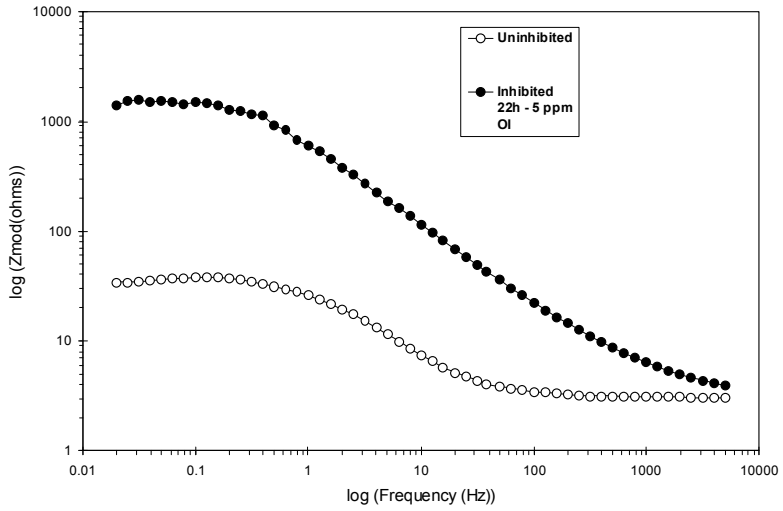

Figure 3.6. Bode plot showing the modulus of the impedance versus frequency for a corrosion test where oleic imidazoline was used as inhibitor.

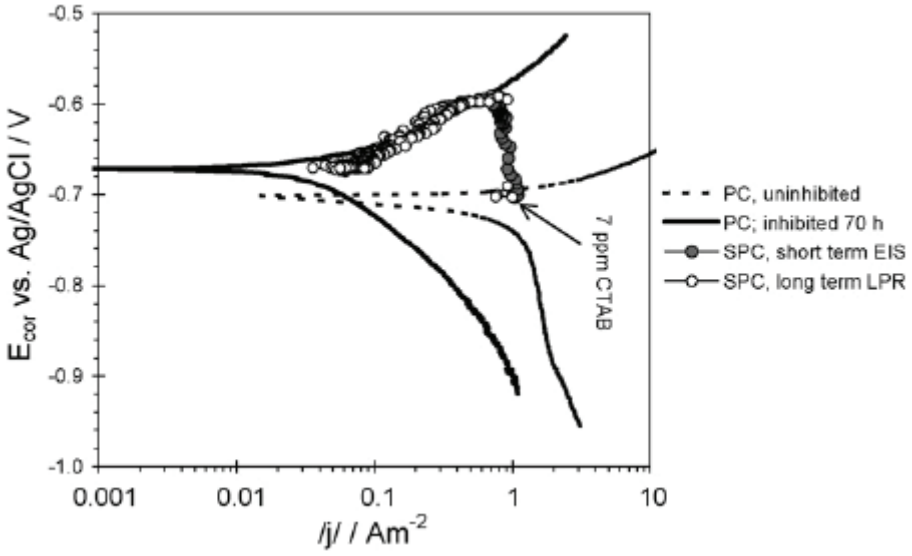

Figure 3.7. E-log|i| plot showing the effect of CTAB addition on the corrosion rate and potential of carbon steel in de-oxygeated brine under 1 bar CO_2.[60]

In Table 3.1 two examples of typical corrosion inhibitor structures is presented. As the chemical structure of the molecules show, a double-bond is seen in the head structure of both inhibitors. As discussed this might increase the possibility of a chemical bonding between the inhibitor head-structure and the steel surface.

Table 3.1. Two typical CO_2 corrosion inhibitor structures, a phosphate ester and an oleic imidazoline.

Oleic imidazoline (OI) (Cationic)	**Phosphate ester (PE) (Anionic)**
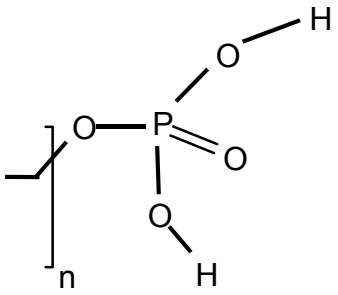	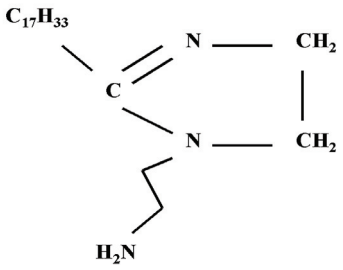

Adsorption and performance of inhibitors might change significantly when certain other chemicals are present in the solution. It has been proven that oil might significantly improve the degree of inhibition. A possible improvement caused by changes in the inhibitor film structure, due to a co-adsorption effect, is thought to be the reason for this effect.[61]

The efficiency of corrosion inhibitors are also affected by the presence of solids on the surface of the steel and the presence of solids or emulsions in the surrounding solution. Adsorption of inhibitor on these surfaces and interfaces might consume the inhibitor and lead to depletion of inhibitor at the steel surface. This might reduce the actual performance of the inhibitor, and might lead to insufficient protection in systems where the bulk concentration of the inhibitor is high enough to ensure protection of bare steel. Typical solids that might affect the performance of the corrosion inhibitor are corrosion product deposits and sand.

3.4.2 pH-stabilization

The modification of fluid phase properties to facilitate iron carbonate precipitation has been used successfully in several gas condensate pipelines in recent years.[63] By adding chemicals that raise the pH of the fluid the corrosion rate can be reduced significantly. Several effects contribute to this reduction in corrosion rate. The reduction in proton concentration following an increase in pH reduces the corrosion rate due to the lower availability of reactants for the cathodic part-reaction. However, as seen in Figure 3.5, the increase in pH greatly affects the solubility of iron carbonate. An adjustment of the system pH might therefore be used to facilitate iron carbonate precipitation, thus precipitating a protective $FeCO_3$ layer on the steel surface. A theoretical overview of the precipitation of iron carbonate and the effect of pH is found in section 3.3. Several papers discussing this technique have been published.[2,63-65]

In section 3.3 the factors affecting the thermodynamics of $FeCO_3$ precipitation were discussed. In systems where the aim is to grow a $FeCO_3$ layer on a steel surface there are other factors that are equally important to the concentration of reactants and the pH. Two such factors are the kinetics of the precipitation reactions and the replenishment of reactants near the steel/$FeCO_3$ surface. To evaluate the probability of sufficient iron

carbonate growth the concept of supersaturation has been introduced. Supersaturation is used to determine if precipitation is energetically favourable given the concentration of ferrous iron and carbonate in the solution. The supersaturation (S) is defined as (3.28):[65]

$$S = \frac{c_{Fe^{2+}} c_{CO_3^{2-}}}{K_{sp}} \tag{3.28}$$

Where c_i is the concentration of the species i and K_{sp} is the solubility product for the precipitate. A supersaturation above 1 means precipitation will occur, thermodynamically. The kinetics of the reactions is not included in the expression for supersaturation. In general the supersaturation needed to obtain a significant precipitation rate is inversely proportional to the temperature. This means that S must be very high in order to get significant precipitation at lower temperatures (<60 °C). The efficiency of the pH stabilization technique to prevent corrosion thus depends on the relationship between the temperature and the continuous supersaturation of reactant near the surface. If the temperature is low the pH must be high enough to maintain the precipitation rate needed to protect the steel surface while it corrodes. By plotting the supersaturation as a function of bicarbonate concentration at a given temperature and Fe^{2+} concentration the strong relationship between pH and supersaturation is seen. This effect is shown in Figure 3.8, where the data proposed by Oddo and Thomson is used to plot bicarbonate concentration and supersaturation versus pH.[66]

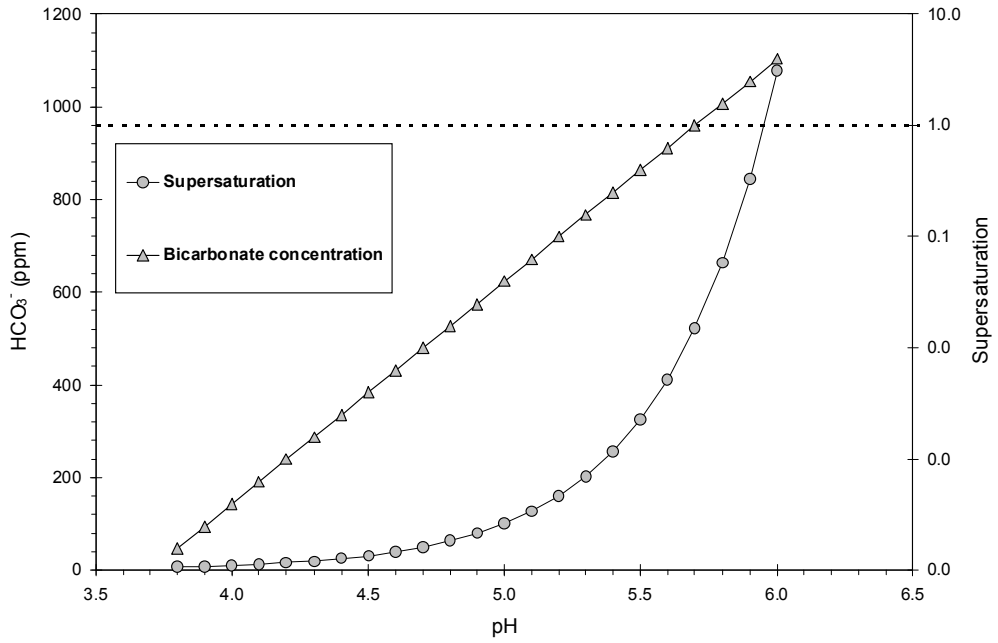

Figure 3.8. Plot of bicarbonate concentration and supersaturation of iron carbonate ($FeCO_3$) as a function of pH. Conditions are 1 bar CO_2, 20 °C, 0.1 Wt% NaCl, 50 ppm Fe^{2+}.

Figure 3.9 sows an example of how a growing ferrous carbonate corrosion product deposit might look like in a solution with mild stirring at 80°C after more than 200 hours of precipitation.

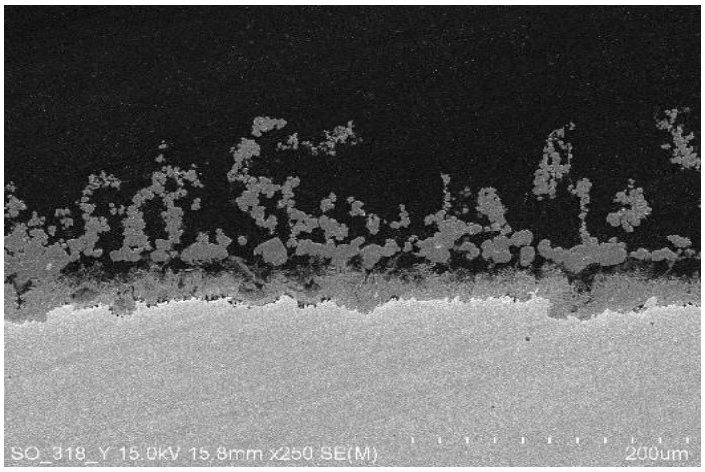

Figure 3.9. Picture of a $FeCO_3$ covered steel surface, Experimental conditions: 80 ºC (0.8 bar CO_2), 3% NaCl, 200 hours of precipitation.

Nesic et al. developed a mechanistic model for uniform CO_2 corrosion of carbon steel. The model is called the scaling tendency model.[65] This model calculates local equilibrium of species and corrosion rate by combining the equations in section 3.2 with equations describing the transport of species in the solution and the potential for each species in solution.

The predictions of the scaling tendency model can be used to decide the probability for a protective scale formation on the steel surface. This means that the results can be placed in either of the two following categories:

- The precipitation and growth rate of the iron carbonate is smaller then the corrosion rate, meaning that complete coverage of the surface (dense layer) is not obtained
- The precipitation and growth rate of the iron carbonate exceeds the corrosion rate of the system, leading to the formation of a dense layer fully covering the steel surface

The reduction in corrosion rate is thus a combination of three factors. 1) The reduction in solution protons available for reduction 2) The reduction of diffusion/convection near the steel surface due to the $FeCO_3$ layer 3) The coverage of the steel surface by iron carbonate attached to the surface. The uniform CO_2 corrosion model proposed by Nesic does not, however, deal with phenomena like spalling, which might occur for systems with a significant flowrate in the fluid stream.[63]

4 Experimental techniques

A short introduction to the main techniques used in the experimental work is given below. The techniques are divided into three sections; electrochemical measurements, contact angle measurements and zetapotential measurements.

4.1 Electrochemical measurements

Several electrochemical techniques were used in the experimental studies. Two methods, polarization resistance and electrochemical impedances spectroscopy, formed the basis for most of the results. A description of the two types of experiments is done in section 4.1. The techniques have a vide variety of applications outside the field of corrosion but only the applicability to corrosion is discussed here. A more detailed review is not in the scope of the work. Several comprehensive descriptions of the methods can be found in the literature.[10,45]

4.1.1 Polarization resistance:

The polarization resistance technique is a widely used electrochemical technique for measuring corrosion rates. It is mainly utilized to measure uniform corrosion as a supplement to or replacement for mass loss measurements.

In a polarization resistance experiment a metallic sample in an electrolyte is subjected to a stepwise potential polarization relative to the corrosion potential. The polarization is measured against a reference electrode, typically an Ag/AgCl electrode. Polarization is achieved by coupling the corroding sample with an external power supply (potentiostat) and a counter electrode made of inert material, e.g. Ti or Pt. The applied potential is then correlated with the measured current to obtain quantitative results for the system. The resulting current is a measure of the rate determining mass transfer or charge transfer rate for the system.[67] The polarization resistance (R_p), which is given by the ratio of potential polarization (∂E) to current response (∂i), is then found for the system.

$$\left[R_p = \frac{\partial E}{\partial i} \right]_{t=0, \Delta E \to 0} \tag{4.1}$$

In the case of small overpotentials, typically ±10 mV, this current response can be linearized; the polarization resistance technique is therefore sometimes also referred to as linear polarization resistance (LPR). The corrosion current density (i_{corr}) can be found from equation 4.2.

$$i_{corr} = \frac{B}{AR_p} \tag{4.2}$$

Where A is the exposed surface area of the test electrode and B is a constant. In the case of simple activation controlled reactions the value of the B can be determined from the Tafel slopes of the anodic and cathodic reactions by equation (4.3).[67]

$$B = \frac{b_a b_c}{2.303(b_a + b_c)} \tag{4.3}$$

Where b_a and b_c are the Tafel slopes of the anodic and cathodic polarization curves, respectively. In actual experiments the polarization resistance (R_p) should be corrected for uncompensated electrolyte resistance (R_u), which can be measured by electrochemical impedance spectroscopy.[67]

In natural environments a perturbation of the potential of up to ±10 mV is considered to be a limiting value due to an increasing deviation from linearity at higher potential polarizations. The scan rate will also affect the mass balance at the surface of the corroding specie. When an optimum scan rate is used the sample is polarized with a minimum capacitative current $C \times (\frac{dv}{dt})$ at each point along the scan. If the scan rate is too fast the amount of current required to hold the potential is too high and the calculated polarization resistance potential is thus too low.[67] The polarization and scan rate are values that need to be optimized for the environment of interest.

In a system where carbonic acid is the dominant corrosive compound there are several issues that must be dealt with. If inhibitors are present, the system can be divided into an uninhibited system and an inhibited system, each exhibiting different properties. For uninhibited CO_2 corrosion the main cathodic reaction is the reduction of carbonic acid (H_2CO_3).[68] Below 50 ºC the limiting factor in this system is the slow formation of H_2CO_3 from dissolved CO_2.[47,69] A gradual transition from this situation to an activation-controlled system can be seen for higher temperatures. Anodic Tafel slopes (b_a) of 40 mV to 60 mV have been reported for this system.[47,69] Empirical values are often used for *B*-values due to the complexity of the polarization curves. B-values of 20±5 mV are typically obtained for the uninhibited system.[47,69] This value is consistent with a b_a value of 40-60 mV and a b_c value approaching infinite. Equation (4.3) then reduces to:

$$B = \frac{b_a}{2.303} \tag{4.4}$$

For inhibited systems the cathodic polarization curve normally exhibit Tafel behaviour with b_c values of about 120 mV.[70] In inhibited systems the conditions near E_{corr} cannot be estimated by extrapolation of the polarization curves for the partial currents at high polarization. This phenomena might be explained by desorption of inhibitor at anodic polarizations.[70] The surface of the steel thus have different properties at high anodic polarization than at the freely corrosion potential. Extrapolation of the cathodic polarization line to E_{corr} must therefore be used to estimate B in these systems, due to the irreversible behaviour of the surface-inhibitor system during anodic polarization. This irreversibility also means that a polarization of only ±5 mV should be used when measuring polarization resistance in inhibited CO_2 corrosion systems.[68]

The corrosion data obtained from PR measurements are usually reported as mm/y where Faraday's law is used to calculate the anodic dissolution according to the anodic dissolution reaction $Fe = Fe^{2+} + 2e^-$. A density of 7.9 g/cm^3 is usually used for carbon steel alloys. Some key assumptions must be made before the PR results can be used (not all of these assumptions are necessary met).

- The corrosion potential must be relatively stable

- The corrosion rate must be uniform. If pitting occurs the total anodic dissolution will be measured but the local corrosion rate (in mm/y) will be significantly higher in the local pits than what the measurements indicate
- The kinetic parameters for the anodic and cathodic reactions should be simple

4.1.2 Electrochemical Impedance Spectroscopy

Electrochemical Impedance Spectroscopy (EIS) is an alternating current technique used to investigate both kinetic and mechanistic phenomena of electrochemical systems.[62] The main advantages of the AC technique in corrosion testing are the ability to obtain mechanistic information of the surface reactions while perturbing the electrochemical system to a minimum extent. This means that the measurements can take place while the system is at steady state.

In corrosion science, EIS involves the study of a potential–current relationship derived from an alternating, sinusoidal, current signal. This signal is typically produced by applying a potential (E) to produce a current. The relationship between these can then be interpreted by describing the signal as the voltage and current relationship of an electronic circuit. The applied, sinusoidal, potential can be represented by (4.5):

$$E = \Delta E \sin \omega t \tag{4.5}$$

Where ω is the angular frequency (=$2\pi f$ where f is the frequency in hertz), E is the instantaneous potential and ΔE is the amplitude. This applied signal then produces a corresponding current response which is also sinusoidal of the same frequency. The signal will however have a different amplitude and phase. This signal can be represented by (4.6):

$$i = \Delta i \sin(\omega t + \varphi) \tag{4.6}$$

The relationship between the applied potential and the current response is known as *impedance.*[62] The impedance, Z, has a magnitude of $\frac{\Delta E}{\Delta i}$ and phase φ and is hence a vector quantity. In electrochemical systems the impedance can be described by modelling the system using electronic circuit elements. Examples of these elements can be resistors, where the impedance is R with a phase angle of 0 and capacitors, where the impedance is

given by $Z = -\left(\frac{1}{j\omega C}\right)$ and the phase angle is 90º, or more complex elements such as Warburg impedance elements.[45] The impedance contributions from resistors lie in the real plane while impedance contributions from capacitor elements lie in the complex plane.[62] A circuit system consisting of a resistor coupled in series with a parallel capacitance and resistance element has proven to be a good representation of a corroding surface. A sketch of the circuit is shown in Figure 4.1.

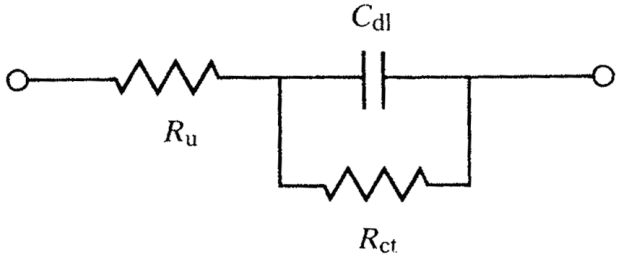

Figure 4.1. Schematic drawing of a circuit system describing a corrosion process.[45]

In Figure 4.1 the resistor and capacitance elements have been labelled according to their relevant physical meaning in an electrochemical system. R_{ct} is the charge transfer resistance. A more general term often used instead of R_{ct} is R_p, polarisation resistance, R_u is the uncompensated (charge transfer) resistance and C_{dl} is the double layer capacitance.

When measuring impedance of a system it is customary to sweep the voltage signal through a range of discrete frequencies. The frequency of the alternating voltage determines which path the current flows through the imaginary electrical circuit used to evaluate the signal. The path can be examined by evaluating the properties of the two parallel elements involved in the diagram in Figure 4.1. When a voltage is applied the reactions on the surface of the electrode will be affected by how long the voltage is perturbed from the open circuit potential of the system. In the case of a capacitor the impedance of the element increases with decreasing frequency. This means that at low frequencies the current will flow through R_p preferentially and at high frequencies through C_{dl} preferentially. This means that the sum of R_u and R_p is measured at zero frequency. At very high frequencies the measured value is then R_u since no ohmic loss is caused by the impedance contribution from C_{dl}. The effects at the high and low frequency ends can be

related to the electrochemical reactions taking place at the electrode surface. R_u is the solution resistance (ohmic loss between the reference electrode and the electrode surface) and may include resistance of surface films and corrosion product layers. R_{ct} (R_p) is the resistance related to the actual electrochemical reaction taking place and is thus essential when studying corrosion phenomena where the resistance to electrochemical reactions might be affected by adsorbents on the surface or changes in the solution chemistry. C_{dl} is in this case a more complex factor; it relates to the capacitance of the double layer and might also be affected by adsorbents changing the electrical double layer at the electrode surface. In systems where the electrochemical reactions are limited by a concentration gradient set up by the consumption of reactants at the high frequencies are limited by a Warburg element. The resulting analysis to find R_p is in this case more complex and a curve fitting method must be used in evaluation of the data.

The data obtained from impedance measurements are typically plotted as either a plot in the complex impedance plane or a plot where the logarithm of the modulus of the total impedance ($log|Z|$) and the phase angle is plotted separately with a common abscissa of log frequency. The total impedance of the system is then given by (4.7).

$$Z(\omega) = Z'(\omega) + jZ''(\omega) \tag{4.7}$$

The latter type plot is called a Bode plot. In a Bode plot a pure resistance is represented by a horizontal line and a constant φ of 0º, while a pure capacitance is a straight line of slope -1 and a φ of -90º. The Bode plot for the circuit given in Figure 4.1 can be seen in Figure 4.2.

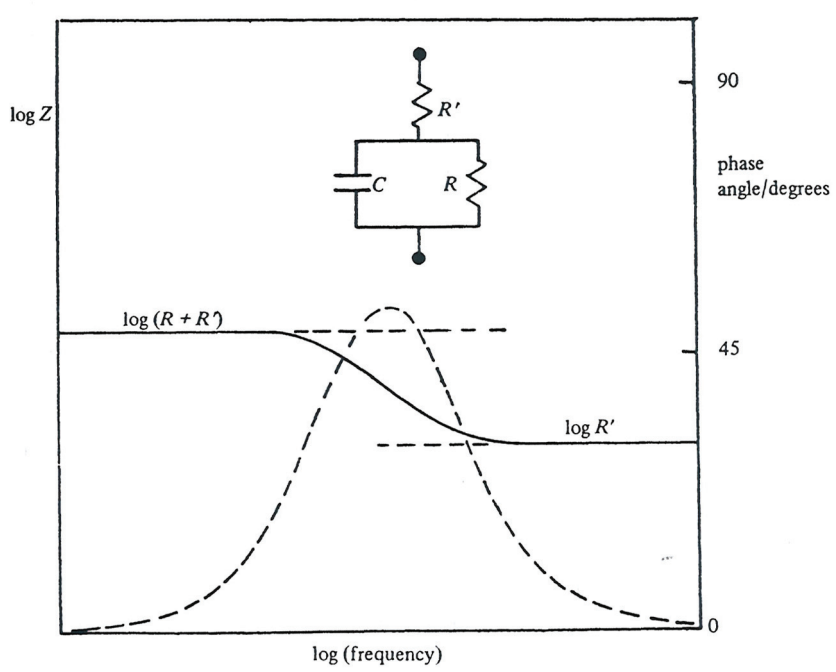

Figure 4.2. Impedance data for the Resistor-Resistor-Capacitor circuit plotted in a Bode plot. The total impedance is plotted as a solid line while the phase angle is plotted as a dotted line.[45]

The instrument software of modern electrochemistry equipment typically provides options to plot the recorded impedance data both in Bode plots and as a plot in the complex impedance plane directly. The evaluation of values such as uncompensated resistance (R_u), polarization resistance (R_p) and capacitance of the system can then be done directly based on the diagrams. The data obtained can then be used to correct or supplement measurements data recorded in polarization resistance measurements or evaluate the properties of the electrode surface.

4.2 Contact angle measurements

There are several techniques that can be used to investigate the interaction between a surface and liquids.[18] Contact angle measurements is one such technique and is well suited for investigating the ability of a liquid to spread on s solid surface (wetting) when the two phases are in contact. When a liquid spread on a substrate (usually a solid), a contact angle (θ) is formed between the liquid and the solid. This is defined as the angle between two of the interfaces at the three-phase line of contact. It must always be stated which interfaces

are used to define θ and in which phase the angle is measured. The contact angle (CA) is thus the angle of the tangent to the curved phase at the contact point with the substrate as shown in Figure 4.3.

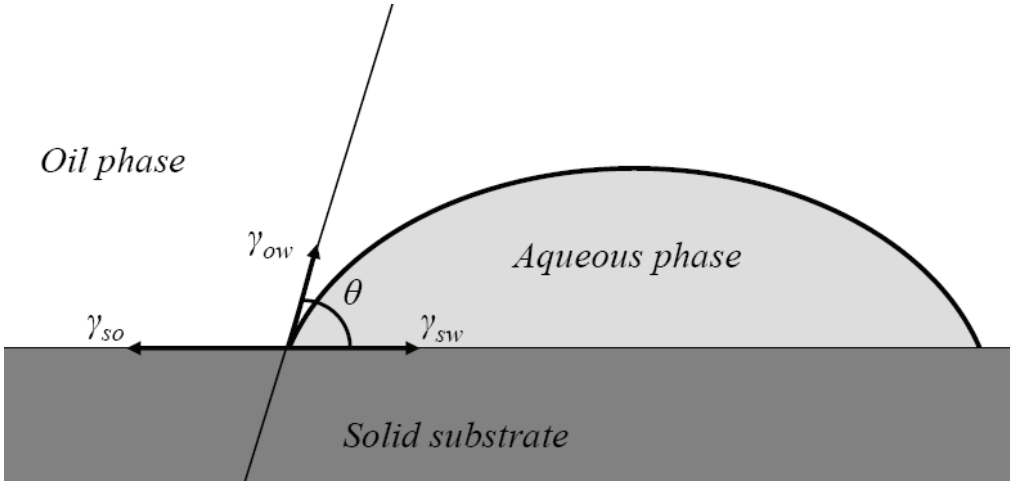

Figure 4.3. Schematic showing the forces acting on the three phase line of contact in a contact angle measurement.

The forces acting on the line of contact between the three phases involved is connected via the Young's equation.

$$\gamma_{sw} = \gamma_{so} + \gamma_{ow} \cos\theta \tag{4.8}$$

where γ is the surface tension between three substances and *s*, *w*, and *o* correspond to the solid, water, and oil substances in a contact angle experiment respectively. This equation assumes a chemically and physically uniform surface which in reality never occurs. The contact angles measured in real experiments are therefore split into an advancing (θ_a) and a receding (θ_r) contact angle.[18]

The most common way to measure the contact angle on a uniform surface is to use a drop-tensiometer. This simple apparatus consists of a light source (preferably monochromatic), support for the sample and a lens system. Pictures are then taken of a droplet deposited on the sample surface. The contact angle can then be assessed directly by measuring the angle formed between the surface and the tangent to the drop surface. In modern drop tensiometers the computer software calculates the contact angle directly.

Several issues has to be considered in real systems where surfaces, such as corroding steel, are used as a substrate for contact angle measurements. Factors such as surface roughness, chemical heterogeneity, sorption layers, molecular orientation and partial solution of the constituent in the substrate, may lead to contact angle hysteresis that complicates the measurements. A corroding substrate might also lead to a similar effect or even a change in the equilibrium contact angle with time. The influence of such factors can be minimized through vibrational methods where vibrations are used to mechanically force the phases to equilibrium. Factors such as surface roughness can also be investigated using environmental scanning electron microscopes where microscopic droplets are condensed onto the relevant surfaces.[71] For iron in CO_2 saturated water the corrosion of the substrate alters might affect the result of the CA measurement by affecting several factors. Liquid composition and precipitation and dissolution of species at the steel surface are two possible processes that may alter conditions for the contact angle measurements. A quantitative analysis of the effect is, however, difficult. In addition to this, experimental problems such as the development of gas bubbles and the development of chemically dissimilar areas of the surface might occur.

4.3 Zetapotential measurements

As discussed in section 2.1.2 the zetapotential (ξ) is the potential at the shear plane of the double layer extending from a solid surface. Several techniques can be used to determine the zetapotential of a surface. The most widely used techniques are electrophoresis measurements and streaming potential measurements.[9] The electrophoresis technique is well suited for measuring particles in suspension due to the development of standardized equipment for this type of measurements. A thorough examination of zetapotential measurements can be found elsewhere.[9]

In a typical electrophoresis experiment a charged particle is moved through a measurement chamber by an applied electrical field. When the dielectric constant of the medium is known, laser Doppler velocimetry can be used to determine the velocity of the suspension moving in the liquid. Laser Doppler velocimetry uses the Doppler effect to measure the velocity: By using radiation from a laser to obtain scattering from the suspensions, a

frequency shift in the radiation is seen.[11] The movement of the particle depend on the charge of the particle, the applied field, the dielectric constant of the medium and the viscosity of the medium. The velocity of the moving particle is then referred to as its electrophoretic mobility (u_e). The electrophoretic mobility and the diffusion coefficient of the suspensions are measured and used to calculate the zetapotential of the suspension. When the mobility, diffusion coefficient and dielectric constant are known the Henry's equation can be used to calculate the zetapotential.

$$u_e = (4\pi\varepsilon_0) \times \frac{D_r \xi}{6\pi} \times f(\kappa a) = \frac{2\varepsilon\xi}{3\eta_v} \times f(\kappa a) \tag{4.9}$$

where D_r is the relative permittivity ($D_r = \frac{\varepsilon}{\varepsilon_0}$), ε is the permittivity of the dielectric, ε_0 is the permittivity of free space and η is the viscosity of the solvent. The factor $f(\kappa a)$ is called Henry's function and is a friction artefact. κ is the Debye-Hückel parameter and depends on the thickness of the double layer while a is the radius of the particles in suspension

Two important approximations of Henry's equation are used in zetapotential measurements. The Smoluchowski equation is a special case where a large particle with a thin double layer moves in a liquid. This system is represented by an aqueous system with a moderate electrolyte concentration. In this case the function $f(\kappa a)$ reduces to (3/2) and a simple relationship can be found.

$$u_e = \frac{2\varepsilon\xi}{3\eta_v} \times f(\kappa a) \approx \frac{\varepsilon\xi}{\eta_v} \tag{4.10}$$

The second approximation can be made for a situation where a small particle with a thick double layer, or a low dielectric constant of the media, moves in a liquid. The function $f(\kappa a)$ then reduces to $f(\kappa a) = 1$ and the Hückel approximation is reached.

$$u_e = \frac{2\varepsilon\xi}{3\eta_v} \times f(\kappa a) \approx \frac{2\varepsilon\xi}{3\eta_v} \tag{4.11}$$

Based on the electrolyte used and the size of the particles one of these approximations is then chosen.

The main difference between iron and most materials previously studied in a CO_2 environment is the instability of the iron surface. The electrochemical reactions on steel are difficult to quantify and the rate of the electrochemical reactions might affect the surface potential of iron. The measured potential might thus be offset by accelerated metal dissolution caused by a potential gradient set up by the electric field in the zetapotential cell. There has been some discussion on these problems by other authors.[72,73] The influence of particle conductivity has also been commented on.[9] The distortion of the applied field by a conducting particle might influence the measured zetapotential for particles fulfilling the prerequisites for using the von Smoluchowski equation ($\kappa a \gg 1$). Metallic dispersions seem to exhibit normal electrophoretic behaviour regardless. Overbeek attributed this behaviour to the effect of polarization.[9] The metallic particle may, in this manner, be treated as an insulator. On aluminium surfaces in an electric field, anodic dissolution of the aluminium at the negative end of the applied field has been reported.[73] The current density is then influenced by the local potential difference between the surface and the solution, as dictated by the electric field. This might also be expected for an actively corroding metal such as iron. The only prerequisite for this type of extra current in an electric field is red-ox reactions taking place at the surface. For the iron surface in an oxygen free environment the red-ox reactions are iron dissolution and reduction of protons. The effect of a red/ox couple in the solution was also confirmed by streaming potential measurements on gold surface.[72] The current from the red/ox couple present in the electrolyte heavily influenced the measured zeta/surface potential in the streaming potential test. A careful approach must therefore be chosen to ensure that the correct zetapotential is measured. Figure 4.4 shows how an applied field might cause a conducting surface to behave like a galvanic cell.

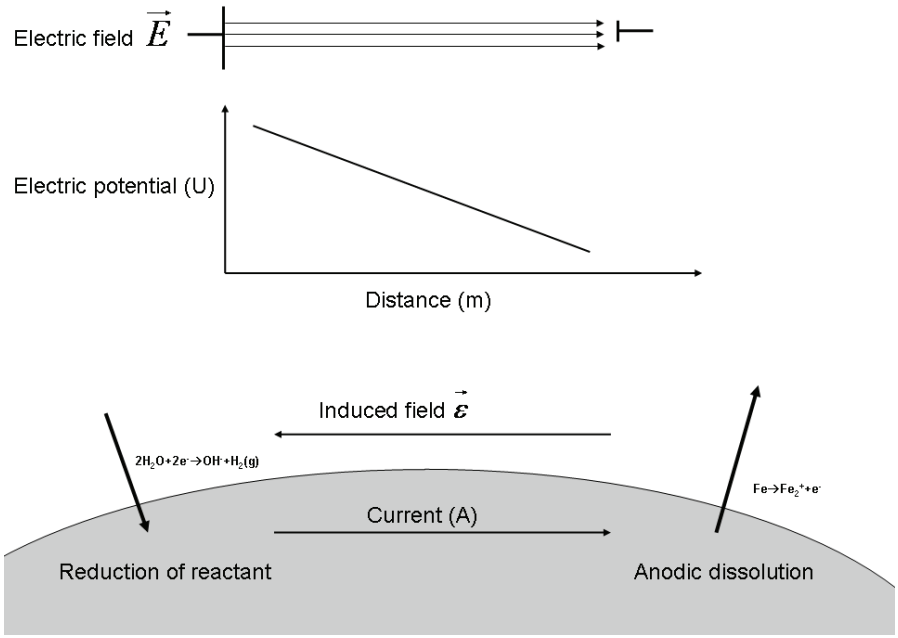

Figure 4.4. Sketch of the electrochemical cell induced by the electric field around a corroding particle. i is the current and U is the potential.

5 Summary of results

5.1 Paper I-III

Papers I-III deal with oil-inhibitor effects on three different types of corroding carbon steel surfaces; I) bare, II) iron carbonate covered and III) covered with ferric corrosion products. Both wetting effects and corrosion inhibitor performance was investigated for the three types of surfaces.

5.1.1 Paper I

The main objective in Paper I was to improve our understanding of the surface chemistry of corroding carbon steel, in particular the interaction between oil, water and corrosion inhibitors on this surface. A particular focus was on the connection between the wetting behavior of the surface and the corresponding CO_2 corrosion rate and inhibition. Contact angle measurements were performed to shed more light on the connection between wettability and corrosion inhibitor additions. In the corrosion experiments the inhibitors were tested with varying degrees of exposure of the specimens to oil. This was done to investigate the effect of oil on inhibitor performance, and effect of oil wetting on the corrosion rate. The choices of inhibitors were based on applicability to real systems and previous knowledge of the inhibitors. Therefore, two commercial corrosion inhibitor base chemicals, a phosphate ester (PE) and an oleic imidazoline salt (OI) and one well-characterized surfactant for reference; cetyl trimethyl ammonium bromide (CTAB), were tested. The three compounds partition towards the water phase at the concentrations used.

The results obtained can be divided into two parts; wetting results and inhibitor performance results. The wetting tests revealed that CTAB acted as a detergent that significantly enhanced water wettability for systems containing CTAB. Both the OI and the PE enhanced the oil wettability of the steel for both oil-in-water and water-in-oil systems, but the effects were only observed for intermediate concentrations in the oil-in-water experiments. An example of the measured contact angles as a function of inhibitor concentration is seen in Figure 5.1. A high contact angle indicates that the surface is hydrophobic.

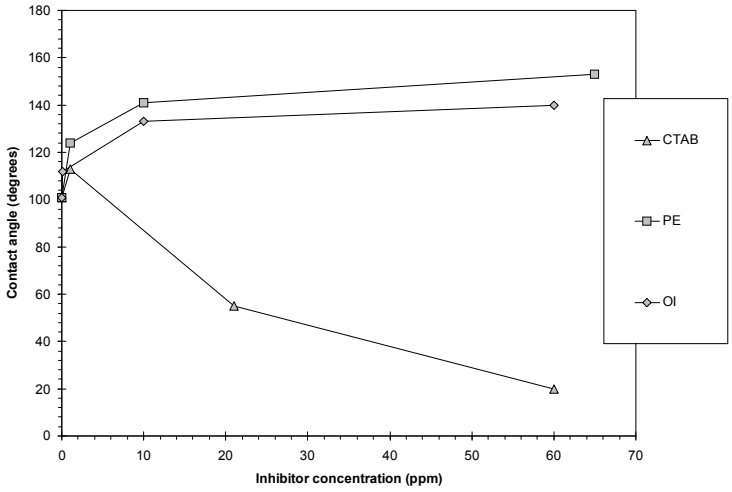

Figure 5.1. Water-in-oil contact angle on precorroded steel surface after 1000 s versus inhibitor concentration for CTAB, PE and OI. Experimental conditions: 1 bar CO_2, 22 ºC, 24 h precorrosion.

The inhibitor performance tests revealed that the performance of the OI and the PE was significantly improved by the presence of oil. The corrosion rates obtained in the tests where oil was added to the brine gave faster and better inhibition of the corrosion. The inhibitor performance improved dramatically after direct exposure to the oil phase. Corrosion rates one order of magnitude lower than in the tests without oil exposure was obtained. The EIS results to be presented indicated that a change in the inhibitor layer and not an oil film leads to the enhanced performance. CTAB did not inhibit the corrosion of the steel in any of the tests conducted. The results obtained in the corrosion inhibitor performance tests are given in Table 5.1. Only the stable corrosion rate obtained for the maximum inhibitor concentration used in the relevant test is included. An indication of the minimum concentration needed to get significant inhibition of the corrosion is also given in the rightmost column.

Table 5.1. Corrosion data obtained in the tests on corroding carbon steel.

	Lowest achievable corrosion rate (mm/y)			**Minimum concentration (ppm) to obtain significant inhibition**		
Inhibitor type	CTAB	OI	PE	CTAB	OI	PE
No oil	-	0.4	0.05	-	3	>10
Oil, no direct exposure	-	0.3	0.06	-	<5	>10
Oil, direct exposure	1	0.02	0.003	-	3	>10

5.1.2 Paper II

The work in Paper II was done to investigate performance of corrosion inhibitors on carbon steel with partly protective $FeCO_3$ deposits in the presence of oil. Alterations in wettability were also investigated by contact angle measurements. The main objective for the work was to obtain a better understanding of how inhibitors interact with an iron carbonate covered steel surface in the presence of oil. The tests were done using the same chemicals as in Paper I.

The wetting experiments revealed that both OI and PE substantially decreased the tendency of water droplets to spread on an initially oil-wet steel surface with $FeCO_3$, but had a negligible effect on the wettability of initially water-wet surfaces. The water-in-oil contact angle measurements indicated that CTAB significantly enhanced water wettability. The measured contact angle as a function of inhibitor concentration for the water-in-oil test is seen in Figure 5.2. It is apparent that addition of OI and PE leads to the same enhanced hydrophobicity seen on carbon steel in Paper I.

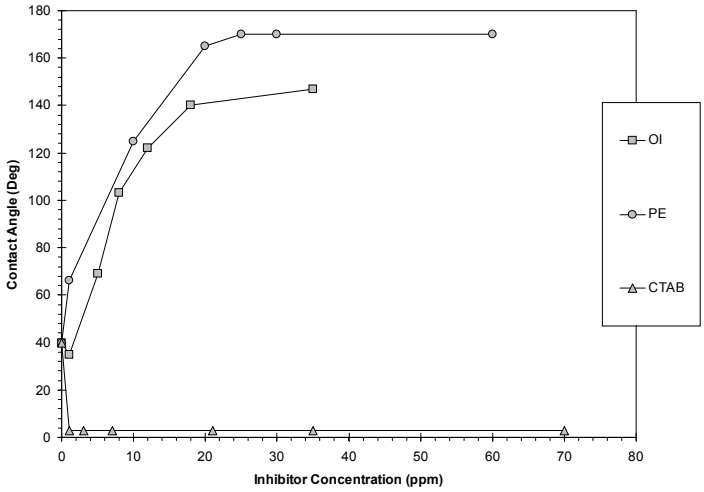

Figure 5.2. Contact angle for water-in-oil experiments steel with $FeCO_3$ deposit. Experimental conditions: 1 bar CO_2, 3% NaCl, and ambient temperature.

A SEM image of a typical $FeCO_3$ covered surface used in the wetting experiments can be seen in Figure 5.3.

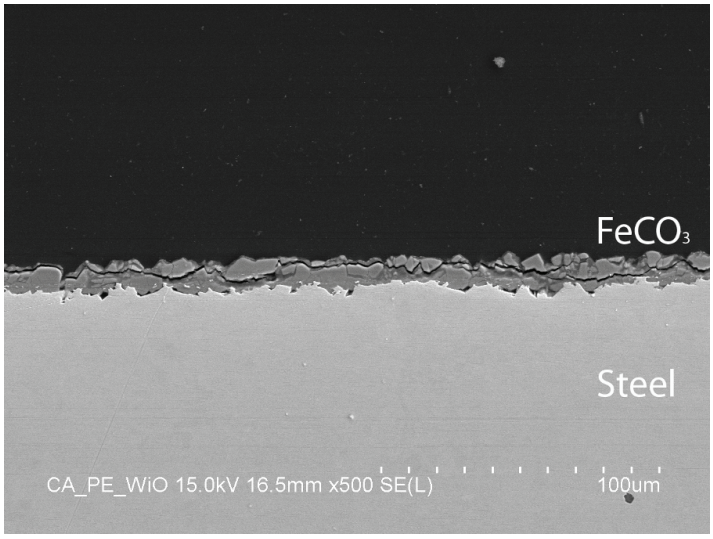

Figure 5.3. SEM picture showing a cross section of a steel specimen with a $FeCO_3$ film used in the contact angle measurements.

Inhibitor performance tests revealed that both OI and PE performance improved in the presence of oil. Corrosion rates one order of magnitude lower than in the tests without oil exposure was obtained. The addition of inhibitor had limited or no effect on the corrosion

rate of steel with $FeCO_3$ deposit in the absence of oil. The results obtained in the corrosion inhibitor performance tests are given in Table 5.2. Only the stable corrosion rate obtained for the maximum inhibitor concentration used in the relevant test is included. An indication of the minimum concentration needed to get significant inhibition of the corrosion is also given in the rightmost column.

Table 5.2. Corrosion data obtained in the tests on corroding carbon steel with $FeCO_3$ deposits.

	Lowest achievable corrosion rate (mm/y)			**Minimum concentration (ppm) to obtain significant inhibition**		
Inhibitor type	CTAB	OI	PE	CTAB	OI	PE
No oil	-	0.2	0.2	-	No effect	No effect
Oil, no direct exposure	0.2	-	-	No effect	-	-
Oil, direct exposure	-	0.03	0.003	-	20	10

Electrochemical impedance spectra (EIS) measurements were conducted to determine if a wetting transition of the $FeCO_3$ surface caused the lowered corrosion rate in systems containing oil. The EIS results indicated that the enhanced performance was caused by a modification of the inhibitor film and not the formation of an oil film on the surface of the steel. A plot of the modulus of the impedance versus frequency is seen in Figure 5.4. The increased uncompensated resistance measured at the high frequency end of the spectra is probably caused by the growth of the iron carbonate layer and not the formation of an oil film.

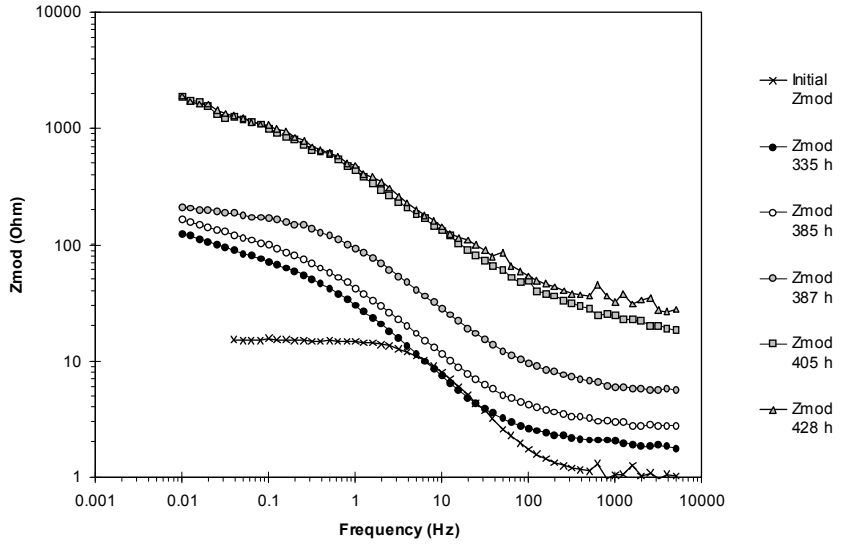

Figure 5.4. Plot showing how the modulus of the impedance (Z_{mod}) versus frequency curve is affected by the growth of a $FeCO_3$ layer and corrosion inhibition by OI at different stages of the experiment with OI and oil exposure.

5.1.3 Paper III

The work in Paper III was conducted to investigate the influence of corrosion inhibitors on the wettability of steel and $FeCO_3$ surfaces exposed to oxygen. The oleic imidazoline and phosphate ester described in Paper I was used in the testing. Two types of surfaces were tested; one precorroded steel surface with ferric corrosion products and one steel surface with $FeCO_3$ deposits which had been exposed to aerated brine. The corrosion and wetting behaviour of the steel was investigated through inhibitor performance tests in CO_2 saturated or aerated brine, and through dispersion and contact angle measurements.

The dispersion and contact angle tests showed that a water-wet to oil-wet transition occurred for the $FeCO_3$ covered steel that had been exposed to aerated brine. In the dispersion tests it was shown that the addition of OI and PE lead to a transition from a preferentially water-wet condition to an intermediate wetting condition at intermediate concentrations of inhibitor. At high concentrations (>100 ppm), PE made the rust particles fully oil-wet in the dispersion tests. The water-wet to oil-wet transition was seen for OI in

the contact angle tests only; this was probably an effect of the longer exposure time in the contact angle experiments.

Inhibitor performance testing revealed that addition of OI enabled the oxidized $FeCO_3$ surface to retain an oil film after exposure to oil. The retained oil film caused a significant drop in corrosion rate in the presence of oxygen. The effect was also seen on a rusting carbon steel surface with ferric corrosion products. No similar effect was seen for PE. A summary of the measured corrosion rates is seen in Table 5.3.

Table 5.3. *Corrosion data obtained in the tests on corroding carbon steel with ferric corrosion products deposits.*

	Lowest achievable corrosion rate (mm/y)		**Minimum concentration (ppm) to obtain significant inhibition**	
Inhibitor type	OI	PE	OI	PE
Oxidized FeCO3	0.03	1	>10	No effect
Oxidized FeCO3 after inhibition	0.006	0.4	-	-
Oxidized carbon steel	0.4	1	15	No effect

Electrochemical impedance measurements were also conducted and a significant shift in mechanism compared to what was seen in Paper I for steel and Paper II or $FeCO_3$ was seen. The EIS data in the high frequency end indicated that a large increase in uncompensated resistance and/or a significantly increased capacitance was seen after exposure to oil, indicating that oil was retained in or at the surface after oil exposure. A plot of the modulus of the impedance versus frequency is seen in Figure 5.5. If the data is compared to the results reported in Papers I-II, it is apparent that the exposure to oil has a significantly different effect on the measured impedance for surfaces exposed to aerated brine.

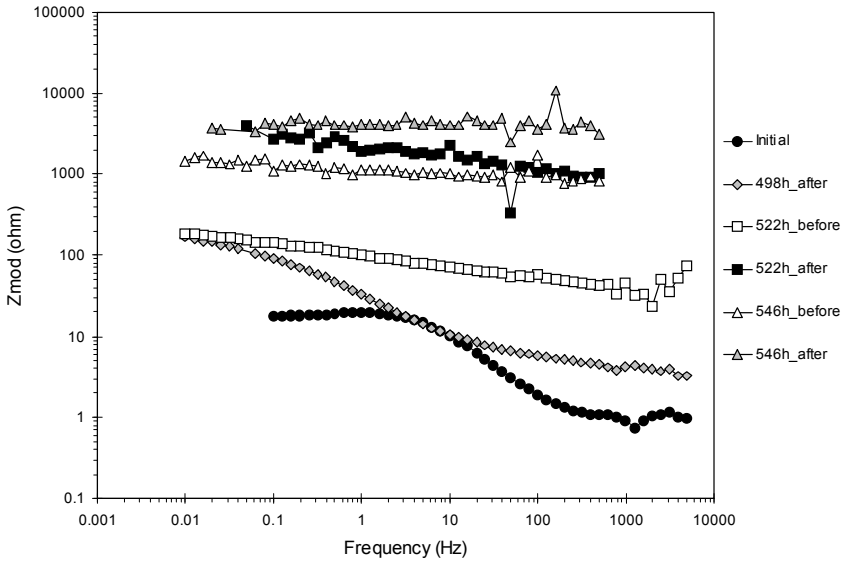

Figure 5.5. Plot showing how the modulus of the impedance (Z_{mod}) versus frequency curve is affected by the growth of a carbonate layer on the steel (up to 498 h) and the retention of an oil film in or on a steel surface (after 522 h) with ferric corrosion products. OI was used as inhibitor.

5.2 Paper IV-V

In Paper IV and V zetapotential measurements were used to investigate adsorption of corrosion inhibitors on $FeCO_3$ and iron particles. The experiments investigated the effect of oil and pH on the zetapotential for the two surfaces. The experiments in Papers IV and V were run at room temperature in a de-oxygenated, 1 bar CO_2 solution.

5.2.1 Paper IV

The background for the investigations in Paper IV was the results obtained in Paper I and II. The interaction between inhibitors and $FeCO_3$ was further investigated by zetapotential measurements in the absence and presence of hydrocarbon oil. The impact of oil on the zetapotential measured after addition of the three inhibitors was also of interest due to the possibility of optimizing the inhibitor adsorption onto a carbonate layer through inhibitor-oil interaction.

The results indicated the all three inhibitor compounds adsorb efficiently and rapidly onto iron carbonate particles. This was seen for tests where the initial zetapotential of the particles was near zero and on surfaces with a positive zetapotential (+30 mV). The positive surface charge prior to inhibitor addition had no apparent effect on the adsorption of the cationic inhibitors. The measured zetapotential did not reveal any effect of oil. The measured zetapotential did not reveal any effect of oil. An isoelectric point (IEP) for iron carbonate was found at pH 6. The zetapotential was found to be positive for pH values below this point and negative for pH values above this point. The determination of the IEP was done by measuring the zetapotential as a function of pH. The IEP is defined as a point at which the zetapotential is zero. At this point the mobility is zero but the actual charge on the particle surface might not be.[74] Figure 5.6 shows the results from the zetapotential-pH plot.

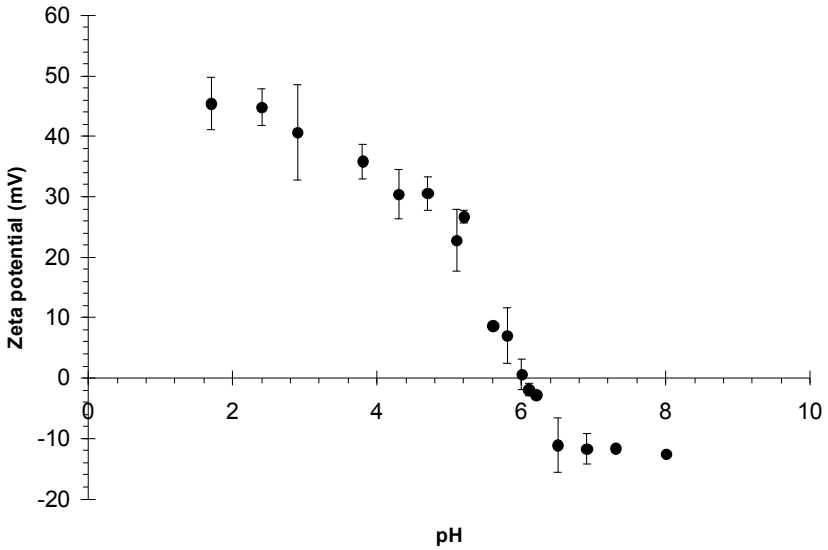

Figure 5.6. Zeta potential of $FeCO_3$ particles as a function of solution pH. Experimental conditions: 22 ^oC, 1 bar CO_2, 0.1% NaCl brine.

Based on the IEP a pH of 5.8±0.2 was chosen as the starting point for the tests with inhibitor. Adsorption of the two cationic (CTAB and OI) and the anionic (PE) inhibitors was then measured through the zetapotential measurements. As expected the zetapotential increased when CTAB and OI was added and decreased when PE was added. Figure 5.7 shows the zeta potential for $FeCO_3$ as a function of OI concentration.

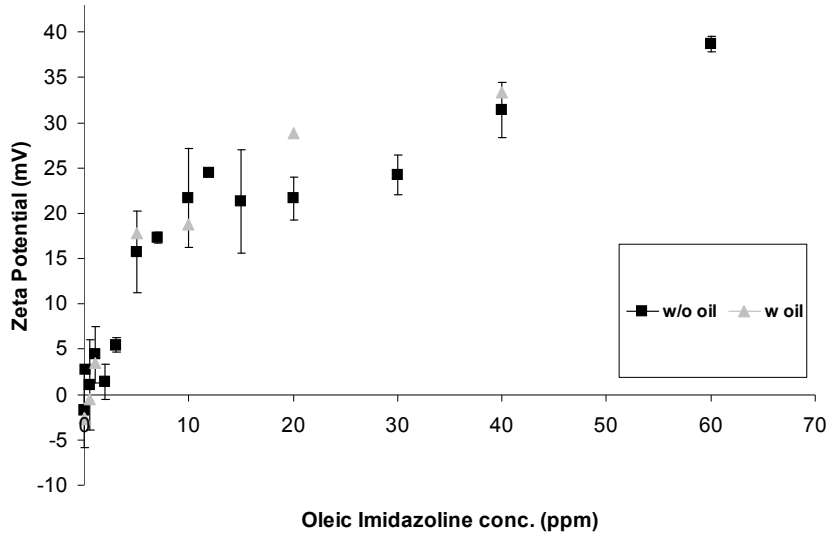

Figure 5.7. Zeta potential off $FeCO_3$ vs. total added concentration of oleic imidazoline product. Experimental conditions: 22 °C, 1 bar CO_2, pH 5.8 ± 0.2, 0.1 Wt% NaCl brine, oil content 2 vol-%.

The measured zetapotential was used to estimate the electrophoretic charge (Q_e) and charge density (σ_e) on the $FeCO_3$ particles. σ_e for CTAB at $FeCO_3$ at two pH values, 4.0 and 6.0, and on oil emulsions at pH 6.0 are plotted in Figure 5.8. σ_e is related to the amount of adsorbed inhibitor on the particles at the different concentrations. In the zetapotential measurements conducted, the only reported charge density is the actual charge density on the shear plane. The measured value might therefore be offset by adsorption of anions inside the shear plane.

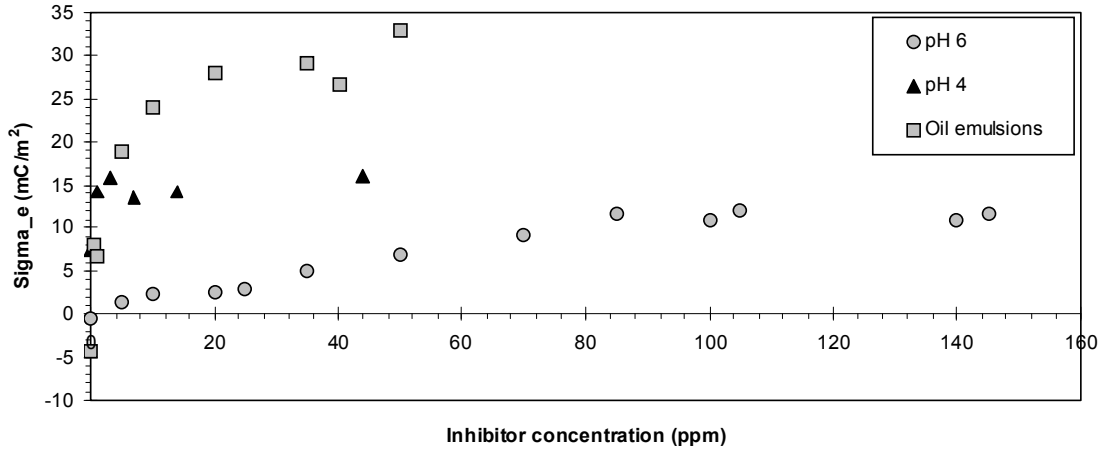

Figure 5.8. Plot of inhibitor concentration versus surface density of charge (σ_e) calculated using equation (3.14).

5.2.2 Paper V

The objectives of the work in Paper V was to determine how the surface potential of corroding iron particles changes with inhibitor concentration and to determine under which conditions determination of the zetapotential was possible. The main task was therefore to develop the experimental methods and investigate the relevance of the obtained results. The effect of pH on the zetapotential of corroding iron particles was also investigated by running the experiments at two different pH values.

It was found that all three inhibitor compounds (CTAB, OI and PE) adsorbed efficiently and rapidly onto the iron particles. The two cationic inhibitors and the anionic inhibitor adsorbed well at both pH 4 and pH 6. The main finding of the paper was that a reproducible zetapotential could be measured for the system when inhibitors were present. The results also indicated that the effect of pH on the change in zetapotential in the presence of increasing levels of inhibitor was present. An example of this is seen in Figure 5.9 below, where PE is used as the added inhibitor.

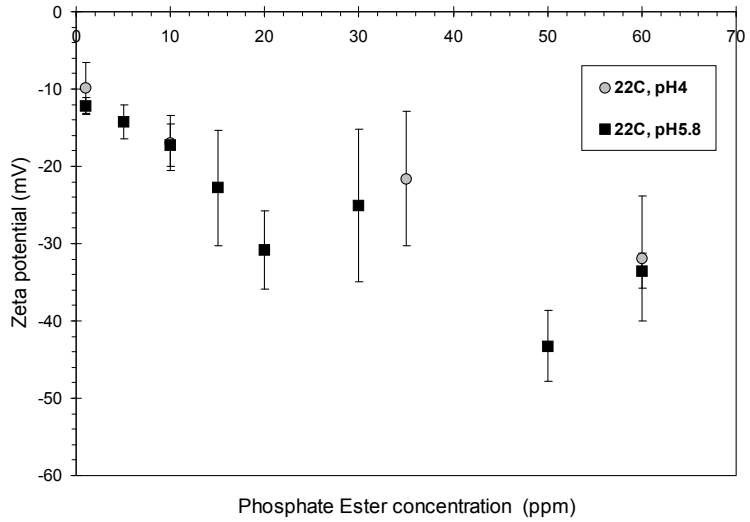

Figure 5.9. The zetapotential on iron particles versus phosphate ester concentration is plotted for tests conducted at pH 4.0 and pH 5.8. Error bars showing the standard deviation for the experiments are included. Experimental conditions: 1 bar CO_2

The results also show that the measured zetapotential in the absence of inhibitor is approximately zero at both pH 4.0±0.2 and pH 5.8±0.2. It is concluded that this might be an artifact caused by the polarization of the electrochemical reactions occurring at the steel surface when placed in an electrical field. The electrochemical reactions provide a low resistance current path that limits the electrokinetic effect. When adding inhibitor, which slows down the electrochemical reaction rates at the steel surface, the resistance of the electrochemical reactions increase, and a zetapotential can be measured. The magnitude of measured potential may still be limited by the presence of the electrochemical reactions.

6 Concluding remarks

The type of corrosion products present on the steel surface has proven to be a key factor in the surface-inhibitor interaction. Both when it comes to the influence of CO_2 corrosion inhibitors on the oil-wettability of the surface and the performance of the inhibitors the nature of the surface is a decisive factor. Through wettability tests the ability of the inhibitors to alter the interaction between oil and bare steel (Paper I), oil and steel with ferrous carbonate deposits (Paper II) and oil and steel with ferric surface deposits (Paper III) were investigated. The results showed that the cetyl trimethyl ammonium bromide surfactant acted as a detergent on both bare steel surfaces and on surfaces with ferrous carbonate deposits. Both the oleic imidazoline and the phosphate ester did, on the other hand, lead to the development of a highly hydrophobic surface when the surface is initially oil-wet. The ability of an oil-wet steel surface to repel water droplets is thus greatly enhanced by these inhibitors thereby reducing the risk of corrosion caused by drop-out of water droplets entrained in the oil. On a water-wet steel surface or on a surface with $FeCO_3$ deposits the inhibitors were not able to affect the wettability substantially. On surfaces with ferric surface deposits the results differed significantly from the other two surfaces. The two CO_2 corrosion inhibitors increased the oil wettability of surfaces with ferric corrosion products even on surfaces that were initially water-wet. The contact angle experiments showed that the addition of OI (>35 ppm) lead to a complete hydrophilic-hydrophobic transition at the surface. A similar although less profound effect was seen for PE.

The inhibitor performance testing revealed that in a system without oil the two corrosion inhibitors did not provide additional protective effect when a partly protective ferrous carbonate layer was present. In tests with oil present the performance increased and the corrosion rate dropped by more than one order of magnitude compared to the system without oil when the samples were directly exposed to oil. This effect was seen on both bare steel and steel with $FeCO_3$ deposits. Partitioning tests revealed that the inhibitors partition strongly to the waterphase. The experiments were also done at concentrations significantly higher than the expected CMC for the inhibitor compounds. Through electrochemical impedance measurements it was determined that the improved effect of the inhibitor seen when oil was present in the solution is caused by a change in the

inhibitor layer (possibly a co-adsorption effect) and not the formation of a hydrocarbon layer on the steel surface. The performance of the inhibitor also improved, although at a slower pace, when the sample was not in direct contact with the oil. The effect of exposure to oil was different for the steel surface with ferric surface deposits. The electrochemical testing was done in aerated brine and revealed that the inhibitors enabled the retention of an oil film on the steel surface after exposure to oil. This oil film was also found to be stable on a time scale of hours. The main findings from the extensive inhibitor performance and surface wettability testing were:

- Addition of oil may strongly influence the inhibitor performance, and is therefore an important factor in inhibitor performance testing.
- Complete transition from water to oil wetting is achievable on steel with ferric corrosion products when OI or PE CO_2 corrosion inhibitors are present.

When investigating the performance of corrosion inhibitors the ability of the inhibitors to adsorb on the surface of the metal where the corrosion is taking place is essential. Through zetapotential measurements it was determined that both the general surfactant, CTAB, and the two corrosion inhibitors adsorb on $FeCO_3$ regardless of surface charge. No significant change in adsorption characteristics could be seen between a surface close to the IEP (pH 5.8±0.2 in 0.1 Wt% NaCl brine and 1 bar CO_2), and a positively charged surface (pH 4.0±0.2). It was also found that the addition of oil had no measurable effect on the zetapotential. On corroding iron particles the focus of the testing was on the feasibility of zetapotential as a characterization technique for the adsorption process. A zetapotential of zero was measured on the iron particles at both pH 4 and at pH 5.8 without inhibitor present. This might be an artifact caused by the electrochemical reactions on the iron surface. The results indicate that measurements on corroding particles, like high purity iron, are complicated by the red/ox reactions initiated by the electrical field used in electrophoretic mobility measurements. Addition of surfactant reduced this effect and lead to a condition where measurements could be made. The change in behavior following inhibitor addition is probably caused by a reduction in the red/ox reaction taking place at the particles surface. At higher concentrations of inhibitor the recorded zetapotential was on a similar magnitude to what was seen on iron carbonate particles.

7 Nomenclature

ε	- Dielectric permittivity	D_r	- Relative permittivity
ρ_v	- Volume density of charge	Q	- Equilibrium constant
e	- Elementary charge	z_i	- Valence of ion
ψ	- Electrostatic potential	ψ_0	- Surface electrostatic potential
ε_0	- Dielectric permittivity of free space	μ_i	- Chemical potential of specie *i*
k	- Boltzmann constant	ψ_{ads}	- Chemical adsorption potential
σ_0	- Surface charge per unit area	ξ	- Zetapotential
r	- Distance from origin	a	- Radius of particle
ξ_r	- Relative zetapotential	σ_e	- Electrokinetic charge density
Qe	- Electrokinetic charge	F	- Faraday constant
I	- Ionic strength	v	- Volume of alkyl chain
l	- Length of alkyl chain	A_h	- Area of headgroup
Γ_i	- Surface excess	c_b	- Bulk concentration
c_i	- Concentration of ion *i*	R	- Gas constant
En^i	- Energy of phase *i*	ΔG	- Gibbs energy
$-\Delta G^0_{ads}$	- Standard energy of adsorption	γ_{AB}	- Interfacial tension
E	- Cell potential	E^{rev}	- Reversible cell potential
E^0	- Standard cell potential at equilibrium	η	- Overpotential
α	- Transfer coefficient	i	- Current density
i_0	- Exchange current density	S	- Supersaturation
K_{sp}	- Solubility product	D	- Diffusion constant
u_e	- Electrophoretic mobility	η_v	- Viscosity of solvent
R_{ct}	- Charge transfer resistance	R_p	- Polarization resistance
R_u	- Uncompensated resistance	C_{dl}	- Double layer capacitance

b_a	- Anodic Tafel slope	b_c	- Cathodic Tafel slope
B	- Tafel slope	C	- Capacitance
Z	- Impedance	φ	- Phase of the impedance
ω	- Angular frequency	θ	- Contact angle

8 Literature

1. M. B. Kermani and A. Morshed, Corrosion **59** (2004), p. 659.
2. A. Dugstad, “Mechanism of Protective Film Formation During CO_2 Corrosion of Carbon Steel”, CORROSION/98, paper no. 31 (Huston, TX: NACE International, 1998).
3. S. Ramachandran, B. Tsai, M. Blanco, H. Chen, Y. Tang and W. A. Goddard, Langmuir **12** (1996), p. 6419.
4. E. Gulbrandsen, R. Nyborg, T. Løland, K. Nisancioglu, “Effect of Steel Microstructure and Composition on Inhibition of CO_2 Corrosion”, CORROSION/2000, paper no. 23, (Houston, TX: NACE International, 2000).
5. I. L. Rozenfield, “Corrosion Inhibitors” New York: McGraw-Hill (1981), p. 67.
6. M. Foss, K. Bilkova, E. Gulbrandsen, M. Knag, J. Sjöblom, Proc. 10th European Symposium on Corrosion Inhibitors, Ann. Univ. Ferrara, N.S., Sez. V, Suppl. N. 12, p. 601 (2005).
7. T. Moon and D. Horsup “Relating Corrosion Inhibitor Surface Active Properties to Field Performance Requirements”, CORROSION/02, paper no. 298, (Houston, TX: NACE International, 2002).
8. B. Alink, B. Outlaw, V. Jovancicevic, S. Ramachandran, S. Campbell, “Mechanism of CO_2 Corrosion Inhibition by The Phosphate Esters”, CORROSION/99, paper no. 37, (Houston, TX: NACE International, 1999).
9. R. J. Hunter, Editors R. H. Otterwill and R. L. Rowell, “Zeta Potential in Colloid Science: Principles and Applications”, London: Academic Press (1981).
10. A. J. Bard, L. R. Faulkner, “Electrochemical Methods; Fundamentals and Applications”, 2nd edition, John Wiley & Sons, Inc. (2001).
11. P. Atkins, J. de Paula, ”Atkins’ Physical Chemistry”, 7th edition, New York: Oxford Univestiy Press, Inc. (2002).
12. E. Kreyzig, “Advanced Engineering Mathemathics”, 8th edition, John Wiley & Sons, Inc. (1999).
13. O. Stern, Electrochemie **30** (1924), p. 508.
14. New Mexico State University, department of Chemistry and biochemistry (www.chemistry.nmsu.edu (2007), accessed 15.12.2008).
15. H. Müller, Kolloidchemie **26** (1928), p. 257.
16. N. E. Hoskin, Transactions of the Faraday Society, **49** (1953), p. 1471.

17. A. L. Loeb, P. H. Wiersema, J. Th. G. Overbeek, “The electrical Double Layer Around a Spherical Colloid Particle”, Cambridge: MIT Press, Mass (1961).

18. D. Fennell Evans and H. Wennerström, “The colloidal domain”, 2nd edition, New York: Wiley-VCH (1999).

19. D. Attwood and A. T. Florence, “Surfactant Systems”, New York: Chapmanand Hall (1983).

20. B. Lindman, H. Wennerström, “Topics in Current Chemistry”, Vol. 87, Berlin: Springer-Verlag (1980).

21. B. P. Binks, Current Opinion in Colloid & Interface Science **7** (2002), p. 21.

22. J. N. Israelachvili, D. J. Mitchell and B. W. B. W. Ninham, Journal of the Chemical Scociety-Faraday Transactions II **72** (1976), p. 1525.

23. K. Holmberg, B. Jönsson, B. Kronberg and B. Lindman, ”Surfactants and Polymers in Aqueous Solution.”, 2nd ed., Chichester: John Wiley & Sons (2003).

24. A. M. Gaudin and D. W. Fuerstenau, Transactions of the American Institute of Mining and Metallurgical Engineers **202** (1955), p. 958.

25. A. P. Robertson and J. O. Leckie, Journal of Colloid and Interface Science **188** (1997), p. 444.

26. S. Paria and K. C. Khilar, Advances in Colloid and Interfaces Science **110** (2004), p. 74.

27. P. Somasundaran and L. Huang, Advances in Colloid and Interface Science **88** (2000), p. 179.

28. D. W. Fuerstenau, “The Adsorption of Surfactants at Solid/Water Interfaces” in the Biochemistry of Biosurfaces vol. 1, editor M. L. Hair, New York: Marcel Dekker (1971), p. 143.

29. E. S. Pagac, D. C. Prieve, R. D. Tilton, Langmuir **10** (1998), p. 2333.

30. A. L. Meader, B. Fries, Industrial and Engineering Chemistry **44** (1952), p. 1636.

31. A. Fava, H. Eyring, Journal of Physical Chemistry **60** (1956), p. 890.

32. M. Gurses, M. Yalcin, C. Sozbilir, Fuel Processes Technology **81** (2003), p. 57.

33. B. H. Bijsterbosch, Journal of Colloid and Interface Science, **47** (1974), p. 186.

34. Y. Gao, J. Du and T. Gu, Journal of the Chemical Society, Faraday Transactions-I **83** (1987), p. 2671.

35. A. Fan, P. Somasundaran and N. J. Turro, Langmuir, **13** (1997), p. 506.

36. P. Somasundaran, J. T. Kunjappu, C. V. Kumar, N. J. Turro and J. K. Barton, Langmuir **5** (1989), p. 215.

37. T. P. Goloub and L. K. Koopal, Langmuir **13** (1997), p. 673.

38. S. U. Pickering, Journal of the Chemical Society **91** (1907), p 2001.

39. D. E. Tambe, M. M. Sharma, Journal of Colloid and Interface Science **157** (1993), p. 244.

40. D. E. Tambe, M. M. Sharma, Advances in Colloid Interface Science **52** (1994), p. 1.

41. N. Yan, M. R. Gray and J. H. Masliyha, Colloids and Surfaces, A: Physicochemical and Engineering Aspects **193** (2001), p. 97.

42. B.P. Binks, D.I. Horsup, J.C. Clark, P.D.I. Fletcher and J.T. Hicks, "I Put it In, but Where Does it Go?-The Fate of Corrosion Inhibitors in Multiphase Systems". CORROSION/07, paper no. 07617, (Huston, TX: NACE International, 2007).

43. M. Foss, E. Gulbrandsen, J. Sjöblom, Corrosion 65 (2009), p. 3.

44. C. Wagner and W. Traud, Zeitschrift für Electrochemie und Angewandte Physicalische Chemie **44** (1938), p. 391.

45. "Instrumental Methods in Electrochemistry", Editors: R. Greef, R. Peat, L. M. Peter, D. Pletcher and J. Robinson, Eastbourne: Horwood Publishing Ltd. (2001).

46. Gulbrandsen, E., Nesic, S., Stangeland, T., Burchardt, B., Hesjevik, S., Skjerve, S., "Effect of Precorrosion on the Performance of Inhibitors for CO_2 Corrosion of Carbon Steel", CORROSION/98, paper no. 013, (Huston TX:NACE International, 1998).

47. S. Nesic, N. Thevenot, J. L. Crolet and D. M. Drazic, "Electrochemical Properties of Iron Dissolution in the Presence of CO_2; Basics Revisited", CORROSION/96, paper no. 3 (Huston, TX: NACE International, 1996).

48. C. de Waard and D. E. Milliams, Corrosion **31** (1975). p. 131.

49. J. O'M. Bockris, D. Drazic and A. R. Despic, Electrochimica Acta **4** (1961), p. 325.

50. S. Nesic, J. Postlethwaite, S. Olsen, "An Electrochemical Model for Prediction of Corrosion of Mild Steel in Aqueous Carbon Dioxide Solutions", CORROSION/96, paper no. 4 (Huston, TX: NACE International, 1996).

51. S. Nesic, J. Postlethwaite, S. Olsen, "An Electrochemical Model for Prediction of CO_2 Corrosion", CORROSION/95, paper no. 131 (Huston, TX: NACE International, 1995).

52. K. Videm, "Progress in the Understanding and Prevention of Corrosion", Proceedings from 10th European Corrosion Congress, (London Institute of Metals, 1993), vol. 1, p. 513.

53. A. Ikeda, M. Ueda and S. Mukai, "CO_2 Corrosion Behaviour and Mechanism of Carbon Steel and Alloy Steel", CORROSION/83, paper no. 45, (Huston, TX: NACE International, 1983).

54. A. Dugstad, L. Lunde and K. Videm, ”Parametric Study of CO_2 Corrosion of Carbon Steel”, CORROSION/94, paper no. 14, (Huston, TX: NACE International, 1994).

55. A. Dugstad, R. Nyborg, M. Seiersten, ”Flow Assurance of pH Stabilized Wet Gas Pipelines”, CORROSION/03, paper no. 03314, (Huston, TX: NACE International, 2003).

56. NACE Glossary of Corrosion Terminology (1965).

57. P. Li, J. Y. Lin, K. L. Tan and J. Y. Lee, Electrochimica Acta **42** (1997): p. 605.

58. S. Meng, E. G. Wang, S. W. Gao, Journal of Chemical Physics **119** (2003), p. 15.

59. H. B. Wang, H. Shi, T. Hong, C. Kang and W. P. Jepson “Characterization of Inhibitor and Corrosion Product Film Using Electrochemical Impedance Spectroscopy (EIS)”, CORROSION/01, paper no. 01023 (Huston, TX: NACE International, 2001).

60. K. Bilkova, E. Gulbrandsen, Electrochimica Acta **53** (2008), p. 5423.

61. M. Foss, E. Gulbrandsen, J. Sjöblom, Corrosion **64** (2008), p. 905.

62. V. S. Sastri, “Corrosion Inhibitors”, West Sussex, England: John Wiley & Sons Ltd. (1998).

63. A. Dugstad and P. Drønen, “Efficient Corrosion Control of Gas Condensate Pipelines by pH-stabilization”, CORROSION/99, paper no. 20 (Huston, TX: NACE International, 1999).

64. S. Nesic, K. J. Lee and V. Ruzic, “A Mechanistic Model of Iron Carbonate Film Growth and the Effect on CO_2 Corrosion of Mild Steel”, CORROSION/00, paper no. 02237 (Huston, TX: NACE International, 2000).

65. S. Nesic, M. Nordsveen, R. Nyborg and A. Stangeland, “A Mechanistic Model for CO_2 Corrosion with Protective Iron Carbonate Films”, CORROSION/01, paper no. 01040 (Huston, TX: NACE International, 2001).

66. J. E. Oddo and M. B. Tomson, Journal of Petroleum Technology **34** (1982), p. 1583.

67. J.R. Scully, Electrochemical Tests; in “Corrosion Tests and Standards”, editor R. Baboian, Philadelphia: American Society for Testing and Materials (1995).

68. E. Gulbrandsen, J. Kvarekvål, H. Miland, Corrosion **61** (2005), p. 1086.

69. S. Nesic, J. Postlethwaite, S. Olsen, Corrosion **52** (1996), p. 280.

70. W.J. Lorenz, F. Mansfeld, Corrosion Science **21** (1981), p. 647.

71. Y. C. Yung and B. Bhushan, Journal of Microscopy **229** (2008), p. 127.

72. J. F. L. Duval, G. K. Hujis, W. F. Threels, Journal of Colloid and Interface Science **260** (2003), p. 95.

73. J. F. L. Duval, Journal of Colloid and Interface Science **269** (2004), p. 211.

74. P. Moulin and H. Roques, Journal of Colloid and Interface Science **261** (2003), p. 115.

Journal Papers I – V are not included due to copyright

1. M. Foss, E. Gulbrandsen, J. Sjöblom, ”Alteration of Wettability of Corroding Carbon Steel Surface by CO2 Corrosion Inhibitors. The Effect on CO2 Corrosion Rate and Contact Angle”, Corrosion 64 (2008), p. 905.

2. M. Foss, E. Gulbrandsen, J. Sjöblom, ”Effect of Corrosion Inhibitors and Oil on Carbon Dioxide Corrosion and Wetting of Carbon Steel with Ferrous Carbonate deposits”, Corrosion 65 (2009), p. 3.

3. M. Foss, E. Gulbrandsen, J. Sjöblom, ”CO2 Corrosion Inhibition and Oil Wetting of Carbon Steel with Ferric Corrosion Products”, Corrosion, Submitted

4. M. Foss, E. Gulbrandsen, J. Sjöblom, ”Adsorption of Corrosion Inhibitors onto Iron Carbonate (FeCO3) Studied by Zetapotential Measurements”, Journal of Dispersion Science and Technology 30 (2009), 10/21.

5. M. Foss, E. Gulbrandsen, J. Sjöblom, ”Measurements of zeta potential on corroding, high-purity iron particles: influence of corrosion inhibitors”, Journal of Dispersion Science and Technology 30 (2009), 10/26.